Journal of the American College of Cardiology
© 2009 by the American College of Cardiology Foundation
Published by Elsevier Inc.

Vol. 53, No. 8, 2009
ISSN 0735-1097/09/$36.00
doi:10.1016/j.jacc.2008.11.014

PRE-CLINICAL RESEARCH

Prolonged Targeting of Ischemic/Reperfused Myocardium by Liposomal Adenosine Augments Cardioprotection in Rats

Hiroyuki Takahama, MD,*†‡ Tetsuo Minamino, MD, PHD,§ Hiroshi Asanuma, MD, PHD,† Masashi Fujita, MD, PHD,§ Tomohiro Asai, PHD,¶ Masakatsu Wakeno, MD, PHD,*†‡ Hideyuki Sasaki, MD,*†‡ Hiroshi Kikuchi, PHD,# Kouichi Hashimoto,** Naoto Oku, PHD,¶ Masanori Asakura, MD, PHD,† Jiyoong Kim, MD,† Seiji Takashima, MD, PHD,§ Kazuo Komamura, MD, PHD,‖ Masaru Sugimachi, MD, PHD,‖ Naoki Mochizuki, MD, PHD,*‡ Masafumi Kitakaze, MD, PHD, FACC†

Osaka, Shizuoka, and Tokyo, Japan

Objectives The purpose of this study was to investigate whether liposomal adenosine has stronger cardioprotective effects and fewer side effects than free adenosine.

Background Liposomes are nanoparticles that can deliver various agents to target tissues and delay degradation of these agents. Liposomes coated with polyethylene glycol (PEG) prolong the residence time of drugs in the blood. Although adenosine reduces the myocardial infarct (MI) size in clinical trials, it also causes hypotension and bradycardia.

Methods We prepared PEGylated liposomal adenosine (mean diameter 134 ± 21 nm) by the hydration method. In rats, we evaluated the myocardial accumulation of liposomes and MI size at 3 h after 30 min of ischemia followed by reperfusion.

Results The electron microscopy and ex vivo bioluminescence imaging showed the specific accumulation of liposomes in ischemic/reperfused myocardium. Investigation of radioisotope-labeled adenosine encapsulated in PEGylated liposomes revealed a prolonged blood residence time. An intravenous infusion of PEGylated liposomal adenosine (450 μg/kg/min) had a weaker effect on blood pressure and heart rate than the corresponding dose of free adenosine. An intravenous infusion of PEGylated liposomal adenosine (450 μg/kg/min) for 10 min from 5 min before the onset of reperfusion significantly reduced MI size (29.5 ± 6.5%) compared with an infusion of saline (53.2 ± 3.5%, $p < 0.05$). The antagonist of adenosine A_1, A_{2a}, A_{2b}, or A_3 subtype receptor blocked cardioprotection observed in the PEGylated liposomal adenosine-treated group.

Conclusions An infusion as PEGylated liposomes augmented the cardioprotective effects of adenosine against ischemia/reperfusion injury and reduced its unfavorable hemodynamic effects. Liposomes are promising for developing new treatments for acute MI. (J Am Coll Cardiol 2009;53:709–17) © 2009 by the American College of Cardiology Foundation

Liposomes are now widely used for drug delivery in cancer treatment to target specific organs actively or passively and to prevent the degradation of chemotherapy agents (1). However, the application of liposomes for cardiovascular diseases is still limited. In ischemic/reperfused myocardium,

See page 718

cellular permeability is enhanced and vascular endothelial integrity is disrupted (2,3), suggesting that nanoparticles

*From the Department of Molecular Imaging in Cardiovascular Medicine, Osaka University Graduate School of Medicine, Osaka, Japan; †Department of Cardiovascular Medicine, National Cardiovascular Center, Osaka, Japan; ‡Department of Structural Analysis, Research Institute, National Cardiovascular Center, Osaka, Japan; §Department of Cardiovascular Medicine, Osaka University Graduate School of Medicine, Osaka, Japan; ‖Department of Cardiovascular Dynamics, Research Institute, National Cardiovascular Center, Osaka, Japan; ¶Department of Medical Biochemistry, School of Pharmaceutical Sciences, University of Shizuoka, Shizuoka, Japan; #Daiichi Pharmaceutical Co., Tokyo, Japan; and the **Daiichi-Sankyo Pharmaceutical Co., Tokyo, Japan. Supported by a grant for Scientific Research and a grant for the Advancement of Medical Equipment from the Japanese Ministry of Health, Labor, and Welfare, as well as a grant from the Japan Cardiovascular Research Foundation.

Manuscript received September 4, 2008; revised manuscript received October 21, 2008, accepted November 3, 2008.

JACC Vol. 53, No. 8, 2009
February 24, 2009:709–17

Abbreviations and Acronyms

8-SPT = 8-(p-sulfophenyl) theophylline

EM = electron microscopy

MI = myocardial infarction

PEG = polyethylene glycol

RI = radioisotope

TTC = triphenyltetrazolium chloride

such as liposomes may be a promising drug delivery system for targeting damaged myocardium with cardioprotective agents. Additionally, coating liposomes with polyethylene glycol (PEG) prolongs their residence time in the circulation (1). Because enhanced microvascular permeability persists for at least 48 h after the occurrence of myocardial infarction (MI) (2), drugs delivered in PEGylated liposomes should be able to display their maximum beneficial effects on myocardial damage after MI.

Adenosine has multiple physiological functions that are mediated via the adenosine A_1, A_{2a}, A_{2b}, and A_3 receptors (4,5). Although large-scale clinical trials suggested the potential value of adenosine therapy for patients with acute MI (6,7), this agent has an extremely short half-life (1 to 2 s) and causes hypotension and bradycardia because of vasodilatory and negative chronotropic effects (4). Because a high dose of adenosine is required to exert cardioprotective effects, it is difficult to use clinically because of the associated hemodynamic consequences. Therefore, we hypothesized that adenosine encapsulated in PEGylated liposomes would cause less hemodynamic disturbance and might also specifically accumulate in ischemic/reperfused myocardium, leading to augmented cardioprotective effects. To test this hypothesis, we created PEGylated liposomal adenosine by the hydration method and investigated: 1) whether liposomal adenosine accumulated in ischemic/reperfused myocardium and prolonged blood residence time; 2) whether liposomal adenosine caused less severe hypotension and bradycardia than free adenosine; and 3) which adenosine receptor subtype was involved in mediating the cardioprotective effects of liposomal adenosine against ischemia/reperfusion injury.

Methods

Materials. The materials for preparing PEGylated liposomes, including hydrogenated soy phosphatidyl choline (HSPC), 1,2-distearoyl-sn-glycero-3-phosphoethanolamine-n-[methoxy (polyethylene glycol)-2000] (DSPE-PEG2000), and cholesterol were obtained from Nissei Oil Co., Ltd. (Tokyo, Japan) and Wako Pure Chemical Co., Ltd. (Osaka, Japan). [^{3}H]-adenosine was purchased from Daiichi Pure Chemicals Co., Ltd. (Tokyo, Japan). Other materials were obtained from Sigma (St. Louis, Missouri), including 8-(*p*-sulfophenyl)theophylline (8-SPT; a nonselective adenosine receptor antagonist), 1,3-diethyl-8-phenylxanthine (DPCPX; a selective adenosine A_1 receptor antagonist), 5-amino-7-(phenylethyl)-2-(2-furyl)-pyrazolo[4,3-e]-1,2,4-triazolo[1,5-c] pyrimidine (SCH58261; a selective adenosine A_{2a} receptor antagonist), 8-[4-[((4-cyanophenyl)carbamoylmethyl) oxy]phenyl]-1, 3-di(n-propyl)xanthine (MRS1754; a selective adenosine A_{2b} receptor antagonist), and 5-propyl-2-ethyl-4-propyl-3-(ethylsulfanylcarbonyl)-6-phenylpyridine-5-carboxylate (MRS1523, a selective adenosine A_3 receptor antagonist).

Animals. Male Wistar rats (9 weeks old and weighing 250 to 310 g, Japan Animals, Osaka, Japan) were used. The animal experiments were approved by the National Cardiovascular Center Research Committee and were performed according to institutional guidelines.

Preparation of PEGylated liposomes. The PEGylated liposomes were prepared by the hydration method. Briefly, adenosine was added to the lipid solution. After mixture of lipid and adenosine, DSPE-PEG2000 was added and incubated. The final composition of PEGylated liposomes was HSPC:cholesterol:DSPE-PEG2000 = 6.0:4.0:0.3 (molar ratio). After ultracentrifugation several times, the pellet of liposomal adenosine was resuspended in sodium lactate at each required concentration for use in the experimental protocols. Some samples of final liposomal adenosine were disrupted by dilution with 50% methanol (1.5 ml per 30-μl of liposomes). After 10 min of ultracentrifugation, the concentration of adenosine in the supernatant was measured by high-performance liquid chromatography.

To prepare fluorescent-labeled liposomes, 0.5 mol% tetramethylrhodamine isothiocyanate (rhodamine) was added to the lipid mixture. To prepare radioisotope (RI)-labeled adenosine encapsulated in liposomes, [^{3}H]-radiolabeled adenosine (Daiichi Pure Chemicals, Tokyo, Japan) was diluted with free adenosine and was encapsulated in liposomes as described above.

Characterization of PEGylated liposomal adenosine. The characterization of the liposomes was performed by the dynamic scatter analysis (Zetasizer Nano ZS, Malvern, Worcestershire, United Kingdom). The analyses were performed 10 times per sample, and results represented analyses of 4 independent experiments.

Experimental protocols. PROTOCOL 1: EFFECTS OF PEGYLATED LIPOSOMAL ADENOSINE ON HEMODYNAMICS IN RATS. Rats were anesthetized with intraperitoneal sodium pentobarbital (50 mg/kg). Catheters were advanced into a femoral artery and vein for the measurement of systemic blood pressure and infusion of drugs, respectively. Both blood pressure and heart rate were monitored continuously during the study using a Power Lab (AD Instruments, Castle Hill, Australia). After hemodynamics became stable, we intravenously administered empty PEGylated liposomes (n = 8), free adenosine (n = 8), or PEGylated liposomal adenosine (n = 8) for 10 min. Either PEGylated liposomal or free adenosine was infused at an initial dose of 225 μg/kg/min (0.1 ml/min) for 10 min. After a 5-min interval, either PEGylated liposomal adenosine or free adenosine was infused at 450 μg/kg/min (0.1 ml/min) for 10 min. In the same manner, PEGylated liposomal adenosine or free adenosine was then infused at 900 μg/kg/min (0.1 ml/min).

PROTOCOL 2: EFFECTS OF PEGYLATED LIPOSOMAL ADENOSINE ON INFARCT SIZE IN RATS. The MI was induced by transient ligation of the left coronary artery as described previously (8). In the first series of experiments, to examine the dose-dependent effects of liposomal adenosine on MI size, PEGylated liposomal adenosine was infused intravenously at 50, 150, or 450 μg/kg/min for a 10-min period starting from 5 min before the onset of reperfusion. In the second series of experiments, to determine the adenosine receptor subtype involved in cardioprotective effects by the liposomal adenosine, the antagonist of adenosine subtype receptor was intravenously injected as a bolus followed by the infusion of liposomal adenosine for 10 min. The MI size was evaluated at 3 h after the start of reperfusion. The doses of adenosine receptor subtype antagonists were determined according to the previous reports (9–11).

Measurement of infarct size. At 3 h after the onset of reperfusion, the area at risk and the infarcted area were determined by Evans blue and triphenyltetrazolium chloride (TTC) staining, respectively, as previously described (8). Infarct size was calculated as [infarcted area/area at risk] × 100(%) in a blind manner. The area at risk was composed of border (TTC staining) and infarcted (TTC nonstaining) areas.

Electron microscopy (EM). Myocardial samples for EM were obtained from the central and peripheral areas in ischemic/reperfused myocardium, which roughly corresponded to the infarcted and border areas, respectively, after the left coronary artery was occluded for 30 min of ischemia followed by 3 h of reperfusion. Samples were prepared as previously reported (12). Liposomes, whose major membrane component is unsaturated phospholipids, were visualized as homogenous dark dots with a diameter of 100 to 150 nm (13).

Accumulation of fluorescent-labeled PEGylated liposomes in ischemic/reperfused myocardium. Unlabeled or fluorescent-labeled PEGylated liposomes were infused intravenously at a dose of 0.1 ml/min as liposomal adenosine was infused in protocol 2. At 3 h after reperfusion, hearts were quickly removed and cut into 4 sections parallel to the axis from base to apex. Then ex vivo bioluminescence imaging was performed with an Olympus OV 100 imaging system (Olympus, Tokyo, Japan) and signals were quantified using WASABI quantitative software (Hamamatsu Photonics K.K., Shizuoka, Japan). Fluorescent intensity in the region of interest was measured as previously reported (14). Control intensity indicated the fluorescent intensity in the nonischemic area of the individual rat.

Time-course changes of free and PEGylated liposomal RI-labeled adenosine in plasma and myocardium. Free or PEGylated liposomal [^{3}H]-adenosine (83 kBq per rat) was infused intravenously at a dose of 0.1 ml/min as liposomal adenosine was infused in protocol 2. At the time indicated, rat hearts were harvested for counting of radioactivity (LSC-3100, Aloka Co., Tokyo, Japan). Results are expressed as a percentage of the injected dose per 1 ml of blood or 1 g of wet tissue weight.

Statistical analysis. The parameters of the liposomes were expressed as the average ± SD, whereas other data were expressed as the average ± SEM. Comparison of time-course changes in hemodynamic parameters between groups was performed by 2-way repeated-measures analysis of variance (ANOVA) followed by a post-hoc Bonferroni test. For comparison of RI activity between groups, statistical analysis was done with the Mann-Whitney *U* test. To address the differences in infarct size among groups, we performed a nonparametric (Kruskal-Wallis) test followed by evaluation with the Mann-Whitney *U* test. Resulting p values were corrected according to the Bonferroni method. To compare parameters of liposomes, an unpaired *t* test was performed. In all analyses, $p < 0.05$ was considered to indicate statistical significance.

Results

Characterization of liposomes by dynamic light scatter analysis. The dynamic light scatter analysis showed no significant difference in mean diameter, polydispersity index, or zeta-potential distribution between empty and adenosine-loaded PEGylated liposomes (Table 1).

Liposomes in ischemic/reperfused myocardium. The EM revealed the intact vascular endothelial cells and cardiomyocytes in the nonischemic myocardium (Figs. 1A and 1B). There were no homogenous dark dots indicating liposomes in the nonischemic myocardium of rats that received either saline (Fig. 1A) or liposomes (Fig. 1B). In the border area, many homogenous dark dots indicating liposomes were accumulated in rats that received liposomes, but not saline (Figs. 1C and 1D). In this area, significant structural damage was not observed in endothelium, but slight swelling of mitochondria was often observed. In the infarcted area, numerous liposomes were detected in rats that received liposomes, but not saline (Figs. 1E and 1F). In this area, the disrupted endothelial integrity and marked swelling of mitochondria were often observed.

Table 1 Characterization of Liposomes by Dynamic Light Scatter Analysis

	Mean Diameter (nm)	Polydispersity Index	Zeta Potential (mV)
PEGylated liposomes (empty liposomes)	126 ± 12	0.035 ± 0.003	−1.7 ± 0.4
PEGylated liposomal adenosine	134 ± 21	0.094 ± 0.002	−2.3 ± 1.1

Results represented analysis of 4 independent experiments. Values are expressed as mean ± SD.
PEG = polyethylene glycol.

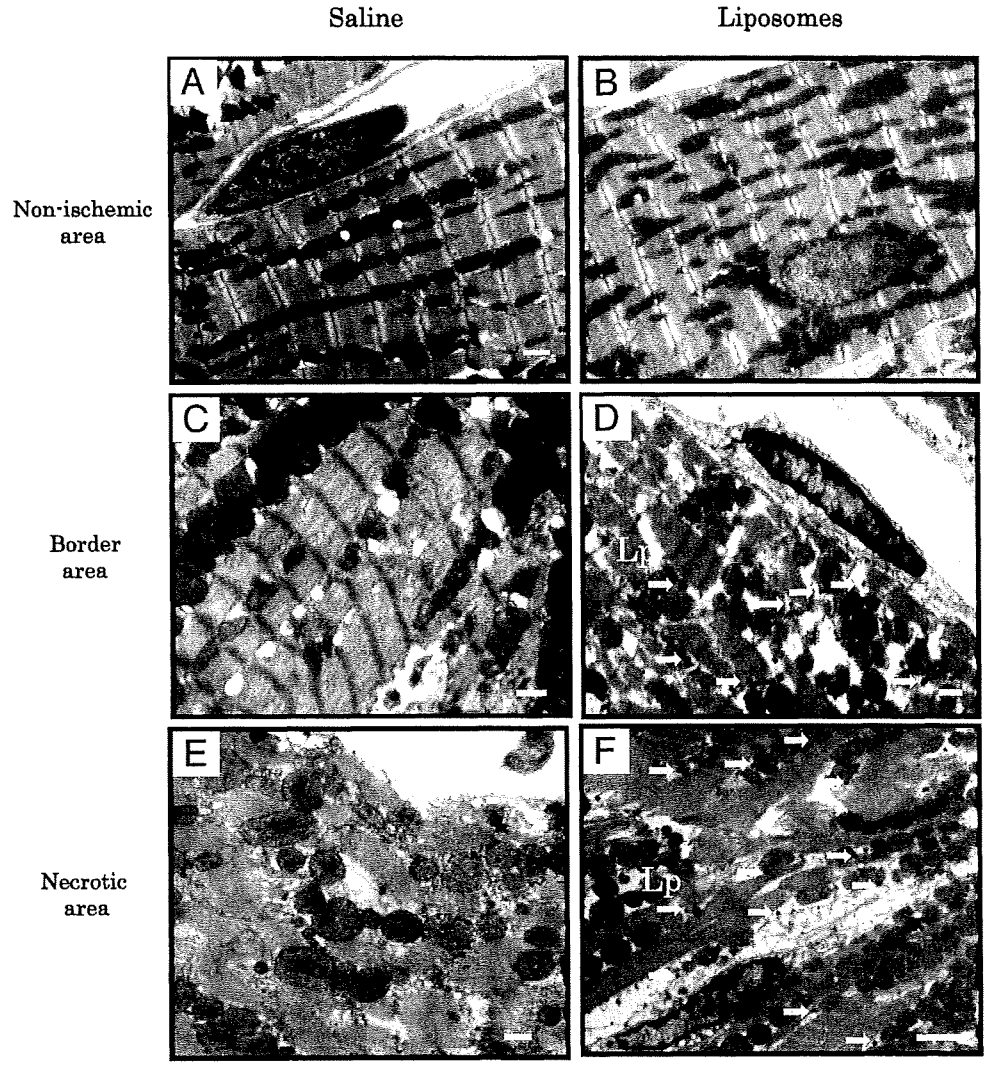

Figure 1 **Liposomes in Ischemic/Reperfused Myocardium**

(A, B) Representative electron micrographs of the nonischemic area in rats that received saline **(A)** or liposomes (Lp) **(B)**. **(C, D)** Representative electron micrographs of border area at 3 h after myocardial infarction (MI). Many **dark dots** accumulated in this area in the rat that received liposomes but not saline. **(E, F)** Representative electron micrographs of infarcted areas at 3 h after MI. Numerous **dark dots** accumulated in this area in the rat that received liposomes but not saline. Scale bars represent 1 μm.

Fluorescent-labeled PEGylated liposomes in ischemic/reperfused myocardium. Quantitative analysis by bioluminescence ex vivo bioluminescene imaging revealed that the target to control fluorescent intensity ratio was higher in the border (noninfarcted area at risk) as well as infarcted areas compared with a nonischemic one, suggesting that fluorescent-labeled liposomes were accumulated in the border as well as infarcted areas. Since there was no high-intensity area when unlabeled liposomes were infused, it was suggested that this was not a nonspecific phenomenon to MI by the ex vivo bioluminescence imaging system (Fig. 2). The Evans blue staining was unrelated to the fluorescence intensity (data not shown).

Plasma radioactivity of RI-labeled adenosine was markedly higher in the PEGylated liposomal adenosine group at 10 min and 3 h after the intravenous infusion than in the free adenosine group (Fig. 3A). Encapsulation within PEGylated liposomes also augmented the accumulation of adenosine in ischemic/reperfused myocardium compared with that of free adenosine (Fig. 3B).

Hemodynamic effects of PEGylated liposomal adenosine. Baseline hemodynamic parameters did not differ among the groups. An intravenous infusion of free adenosine at doses of 225, 450, and 900 μg/kg/min decreased the mean blood pressure by 14.8%, 25.4%, and 33.7%, respectively, compared with the effect of empty PEGylated lipo-

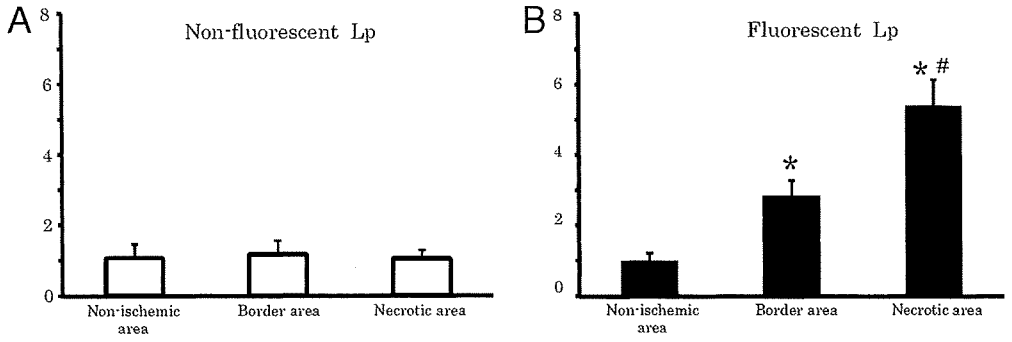

Figure 2 **Detection of Fluorescence-Labeled PEGylated Liposomes in Ischemic/Reperfused Myocardium**

Quantitative analysis of target-to-control fluorescent intensity ratio for each area in rats (n = 3 each group) that received nonfluorescent **(A)** or fluorescent **(B)** liposomes. The values of bioluminescence signals in the border and infarcted areas were expressed as the fold to that of the each nonischemic area. Values are expressed as the mean ± SEM (error bars). *p < 0.05 versus nonischemic areas. #p < 0.05 versus border areas.

somes. In contrast, the intravenous infusion of PEGylated liposomal adenosine at a dose of either 225 or 450 μg/kg/min did not significantly alter mean blood pressure (Fig. 4). Changes of the heart rate after infusion of PEGylated liposomal adenosine or free adenosine were similar to those observed for mean blood pressure (Fig. 4).

Effects of PEGylated liposomal adenosine on MI size. Baseline hemodynamic parameters were similar among all of the groups (Table 2). Intravenous infusion of free adenosine for 10 min reduced both the blood pressure and the heart rate, although these parameters returned to baseline within 5 min of ceasing infusion (Table 2). In contrast, hemodynamic parameters of the other groups were not altered (Table 2). The area at risk in the control group (61 ± 3%) did not differ compared with those of other groups that received liposomal adenosine. Intravenous infusion of PEGylated liposomal adenosine caused a dose-dependent decrease of MI size compared with that in the control group, whereas intravenous infusion of empty PEGylated liposomes or free adenosine did not (Fig. 5B).

The bolus injection of adenosine receptor antagonist did not alter the hemodynamic parameters (Table 3). The area at risk in the liposomal adenosine group (58 ± 3%) did not differ compared with those of other groups that received adenosine receptor antagonist. Infusion of 8-SPT, a nonspecific adenosine receptor antagonist, blunted the cardioprotective effect of liposomal adenosine (Fig. 6B). Furthermore, the infusion of the adenosine A_1, A_{2a}, A_{2b}, or A_3 receptor antagonist also blunted cardioprotective effects of liposomal adenosine (Fig. 6B). Infusion of 8-SPT alone did not significantly affect myocardial infarct size compared with the control (52 ± 5%, n = 4).

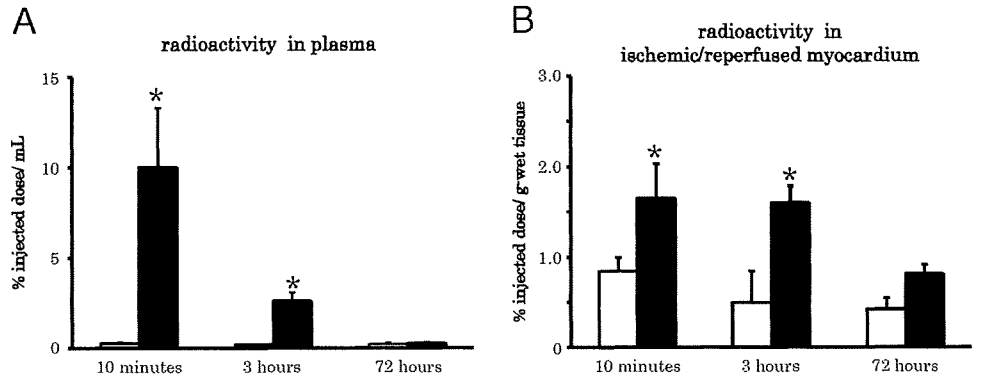

Figure 3 **Radioisotope-Labeled Adenosine in Plasma and Ischemic/Reperfused Myocardium**

(A) Changes in plasma radioactivity after infusion of radioisotope-labeled adenosine. **Solid and open bars** indicate the PEGylated liposomal adenosine and free adenosine groups, respectively (n = 4 each). In the PEGylated liposomal adenosine group, plasma radioactivity was markedly higher than in the free adenosine group. **(B)** Changes in radioactivity in ischemic/reperfused myocardium. **Solid and open bars** indicate the PEGylated liposomal adenosine and free adenosine groups, respectively (n = 4 each). In the PEGylated liposomal adenosine group, myocardial radioactivity was markedly higher than in the free adenosine group. Values are expressed as the mean ± SEM (error bars). *p < 0.05 versus the free adenosine group at the corresponding time.

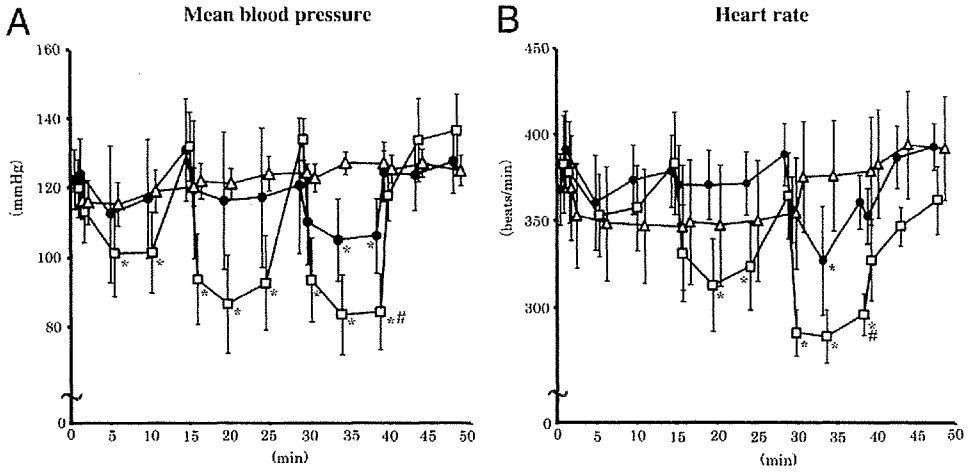

Figure 4 Hemodynamic Effects of PEGylated Liposomal Adenosine

Changes in the mean blood pressure **(A)** and heart rate **(B)** after intravenous infusion of various doses of empty PEGylated liposomes **(triangles)**, PEGylated liposomal adenosine **(circles)**, or free adenosine **(squares)** (n = 8 each). Values are expressed as the mean ± SEM. *p < 0.05 versus baseline at the corresponding group. #p < 0.05 versus PEGylated liposomes.

Discussion

In the present study, EM, bioluminescence ex vivo imaging, and fluorescent analysis revealed the accumulation of liposomes in the border (noninfarcted areas at risk) as well as infarcted ones, but not nonischemic myocardium, at 3 h after MI. These findings suggested that liposomes could specifically accumulate in ischemic/reperfused myocardium. Interestingly, EM revealed the existence of liposomes at sites where endothelial integrity was still morphologically maintained. Endothelial dysfunction such as enhanced permeability is induced by ischemic insult without morphological endothelial disruption (3,15). Enhanced permeability might lead to the accumulation of liposomes in the border as well as infarcted area, which will contribute to salvage the ischemic/reperfused myocardium. However, further investigation will be needed to determine the precise mechanism by which liposomes accumulate in ischemic/reperfused myocardium.

Analysis using RI-labeled adenosine encapsulated in liposomes revealed that plasma radioactivity was markedly higher in the PEGylated liposomal adenosine group compared with the free adenosine group. This indicates that encapsulation of adenosine by PEGylated liposomes considerably prolonged its residence time in the circulation and delayed its degradation. Consistent with the histological data, RI-labeled adenosine also showed preferential accumulation in ischemic/reperfused myocardium.

Table 2 Effects of Liposomal Adenosine on Hemodynamic Parameters

		Ischemia				Reperfusion	
	Baseline	0 min	15 min	25 min	30 min	5 min	10 min
Mean blood pressure (mm Hg)							
Saline	122 ± 5	102 ± 10	108 ± 7	107 ± 9	108 ± 7	105 ± 9	104 ± 9
Vehicle	127 ± 4	109 ± 8	108 ± 7	111 ± 9	111 ± 5	105 ± 5	103 ± 5
Free-Ado	124 ± 8	115 ± 8	111 ± 5	109 ± 4	66 ± 4*	62 ± 4*	112 ± 6
Lp-Ado 50 μg/kg/min	121 ± 5	106 ± 6	105 ± 6	110 ± 10	102 ± 6	101 ± 6	104 ± 4
Lp-Ado 150 μg/kg/min	122 ± 3	107 ± 6	107 ± 6	109 ± 11	105 ± 6	100 ± 6	103 ± 4
Lp-Ado 450 μg/kg/min	124 ± 3	104 ± 6	105 ± 6	107 ± 5	102 ± 6	99 ± 6	104 ± 4
Heart rate (beats/min)							
Saline	363 ± 22	366 ± 19	369 ± 14	413 ± 22	372 ± 12	372 ± 16	371 ± 14
Vehicle	363 ± 32	363 ± 6	383 ± 6	396 ± 25	367 ± 6	374 ± 7	372 ± 7
Free-Ado	360 ± 18	361 ± 17	384 ± 13	379 ± 18	305 ± 11*	293 ± 13*	356 ± 14
Lp-Ado 50 μg/kg/min	378 ± 19	386 ± 21	366 ± 12	376 ± 12	367 ± 19	369 ± 9	377 ± 17
Lp-Ado 150 μg/kg/min	388 ± 27	376 ± 20	371 ± 14	377 ± 13	378 ± 16	373 ± 16	369 ± 17
Lp-Ado 450 μg/kg/min	368 ± 17	376 ± 21	361 ± 13	386 ± 15	368 ± 15	363 ± 6	367 ± 7

Values are expressed as mean ± SEM. *p < 0.05 versus baseline.
Free-Ado = free adenosine; Lp-Ado = PEGylated liposomal adenosine; PEG = polyethylene glycol; vehicle = PEGylated liposomes.

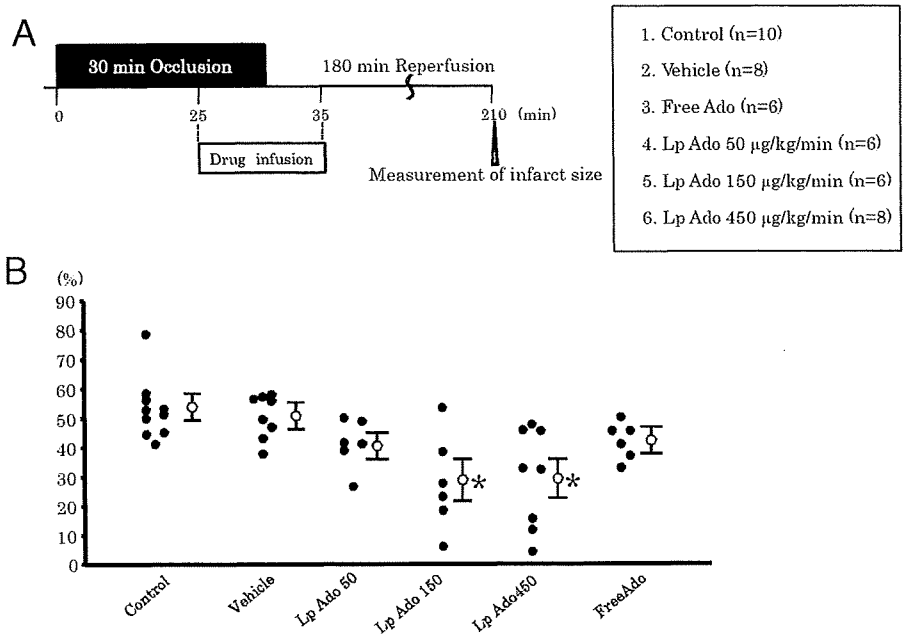

Figure 5 Dose-Dependent Effects of PEGylated Liposomal Adenosine on Myocardial Infarct Size

(A) Protocol showing the timing of infusion of PEGylated liposomal adenosine and of infarct size measurement. **(B)** Myocardial infarct size. Values are expressed as mean ± SEM (error bars). *p < 0.05 versus the control group. Free-Ado = free adenosine; Lp-Ado = PEGylated liposomal adenosine; Vehicle = PEGylated liposomes.

Furthermore, this study showed that PEGylated liposomal adenosine had a weaker effect on the blood pressure and heart rate than free adenosine. Thus, encapsulating adenosine in PEGylated liposomes attenuated its vasodilatory and negative chronotropic effects, presumably by reducing the amount of circulating free adenosine. However, the changes of hemodynamic parameters in this in vivo model suggested that significant release of adenosine from PEGylated liposomes would still occur if a large dose of liposomal adenosine (e.g., 900 μg/kg/min) were administered. Thus, further investigation of the in vivo pharmacodynamics of PEGylated liposomal adenosine is needed.

An intravenous infusion of PEGylated liposomal adenosine at the maximum dose that did not disturb hemodynamic parameters for 10 min before reperfusion reduced MI size in a dose-dependent manner, and this improvement was blocked by 8-SPT, a nonselective adenosine receptor antagonist. These findings suggest that adenosine released from liposomes acts via an adenosine receptor-dependent pathway. One possible mechanism by which PEGylated lipo-

Table 3 Effects of Adenosine Receptor Antagonist on Hemodynamic Parameters

		Ischemia				Reperfusion	
	Baseline	0 min	15 min	25 min	30 min	5 min	10 min
Mean blood pressure (mm Hg)							
Lp-Ado + 8SPT	120 ± 6	113 ± 4	112 ± 6	112 ± 5	107 ± 6	102 ± 8	109 ± 7
Lp-Ado + DPCPX	130 ± 6	105 ± 4	121 ± 4	100 ± 10	122 ± 6	120 ± 6	111 ± 4
Lp-Ado + SCH58261	132 ± 2	98 ± 12	99 ± 8	110 ± 8	118 ± 10	113 ± 10	109 ± 6
Lp-Ado + MRS1754	130 ± 3	95 ± 12	106 ± 8	105 ± 10	100 ± 10	96 ± 10	99 ± 7
Lp-Ado + MRS1523	130 ± 2	109 ± 8	104 ± 8	105 ± 9	100 ± 9	101 ± 10	104 ± 6
Heart rate (beats/min)							
Lp-Ado + 8SPT	404 ± 17	385 ± 10	374 ± 8	396 ± 8	389 ± 9	383 ± 8	385 ± 9
Lp-Ado + DPCPX	396 ± 24	380 ± 11	399 ± 9	398 ± 12	385 ± 9	382 ± 9	380 ± 7
Lp-Ado + SCH58261	393 ± 14	399 ± 15	381 ± 9	395 ± 15	376 ± 9	373 ± 9	385 ± 7
Lp-Ado + MRS1754	398 ± 14	392 ± 11	401 ± 9	379 ± 15	378 ± 9	374 ± 9	377 ± 7
Lp-Ado + MRS1523	396 ± 9	390 ± 11	390 ± 11	392 ± 10	373 ± 9	391 ± 7	388 ± 11

Values were expressed as mean ± SEM. *p < 0.05 versus baseline.
Lp-Ado = PEGylated liposomal adenosine; PEG = polyethylene glycol; Vehicle = PEGylated liposomes.

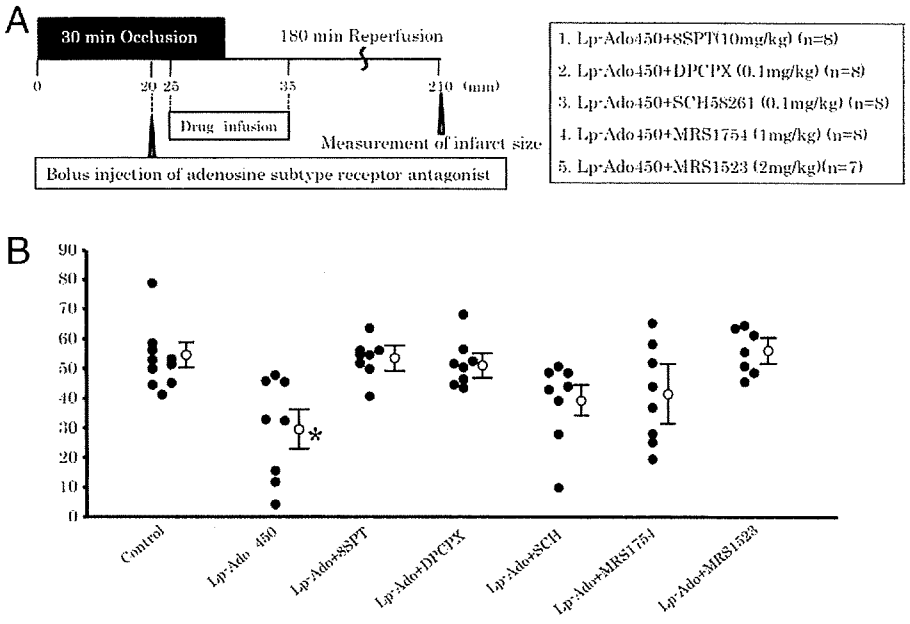

Figure 6 **Effects of Adenosine Receptor Antagonists on Myocardial Infarct Size**

(A) Protocol showing the timing of infusion of PEGylated liposomal adenosine and bolus injection adenosine receptor antagonists. **(B)** Myocardial infarct size. Values are expressed as the mean ± SEM (error bars). *$p < 0.05$ versus the control group. The abbreviations for adenosine antagonists were described in the text. Abbreviations as in Figure 5.

somes could augment cardioprotective effects of liposomal adenosine with minimum effects on hemodynamic parameters is the enhanced accumulation of PEGylated liposomal adenosine in ischemic/reperfused myocardium, which could augment various beneficial actions such as preventing calcium overload in the myocardium (5). The prolonged persistence of PEGylated liposomal adenosine would also increase its beneficial effect on ischemic/reperfused myocardium. Although continuous high-dose, long-term infusion of free adenosine was reported to reduce infarct size in rats (16), the present study did not confirm such a cardioprotective effect, probably because the total dose of free adenosine that we used was not high enough.

We found that myocardial infarct size in the group that received PEGylated liposomal adenosine with the antagonist of adenosine A_1, A_{2a}, A_{2b}, or A_3 subtype receptor was no different from the control group, indicating that every adenosine subtype receptor could possibly play a role in mediating cardioprotection by liposomal adenosine and that it was difficult to identify one particular subtype in the present study. Numerous studies reported that A_1, A_{2a}, A_{2b}, and A_3 receptors have been involved in cardioprotection against ischemia/reperfusion injury, and it remains controversial which adenosine subtype receptor is most responsible for cardioprotection (17–20). Furthermore, because the adenosine receptor antagonists used in the present study had some nonspecific effects, future investigation will be needed to examine the precise role of each adenosine receptor subtype using genetically engineered mice.

Because liposomal adenosine infused during reperfusion could reduce MI size, this agent could be a candidate for the adjunctive therapy of patients with acute MI. Importantly, adenosine is currently used for the diagnosis of ischemic heart disease and PEGylated liposomes are used to deliver anticancer agents (21). Thus, it should not be difficult to introduce PEGylated liposomal adenosine into clinical practice. Finally, PEGylated liposomes may provide a useful drug delivery system for targeting ischemic/reperfused myocardium with other agents.

Acknowledgments

The authors thank Akiko Ogai and Yoko Nakano for their excellent technical assistance; Motohide Takahama, Hiroyuki Hao, and Hatsue Ishibashi-Ueda for advice about the electron microscopy figure; and Syunichi Kuroda and Takashi Matsuzaki for assistance with bioluminescence imaging.

Reprint requests and correspondence: Dr. Tetsuo Minamino, Department of Cardiovascular Medicine, Osaka University Graduate School of Medicine, 2-2 Yamadaoka, Suita, Osaka 565-0871, Japan. E-mail: minamino@medone.med.osaka-u.ac.jp.

REFERENCES

1. Papahadjopoulos D, Allen TM, Gabizon A, et al. Sterically stabilized liposomes: improvements in pharmacokinetics and antitumor therapeutic efficacy. Proc Natl Acad Sci U S A 1991;24:11460–4.

2. Horwitz LD, Kaufman D, Keller MW, Kong Y. Time course of coronary endothelial healing after injury due to ischemia and reperfusion. Circulation 1994;90:2439–47.
3. Dauber IM, Van Benthuysen KM, McMurtry IF, et al. Functional coronary microvascular injury evident as increased permeability due to brief ischemia and reperfusion. Circ Res 1990;66:986–98.
4. Forman MB, Stone GW, Jackson EK. Role of adenosine as adjunctive therapy in acute myocardial infarction. Cardiovasc Drug Rev 2006;24: 116–47.
5. Mubagwa K, Flameng W. Adenosine, adenosine receptors and myocardial protection: an updated overview. Cardiovasc Res 2001;52:25–39.
6. Mahaffey KW, Pume JA, Barbagelata NA, et al. Adenosine as an adjunct to thrombolytic therapy for acute myocardial infarction: results of a multicenter, randomized, placebo-controlled trial: the Acute Myocardial Infarction STudy of ADenosine (AMISTAD) trial. J Am Coll Cardiol 1999;34:1711–20.
7. Ross AM, Gibbons RJ, Stone GW, Kloner RA, Alexander RW, for the AMISTAD-II ÅInvestigators. A randomized, double-blinded, placebo-controlled multicenter trial of adenosine as an adjunct to reperfusion in the treatment of acute myocardial infarction (AMISTAD-II). J Am Coll Cardiol 2005;45:1775–80.
8. Bullard AJ, Govewalla P, Yellon DM. Erythropoietin protects the myocardium against reperfusion injury in vitro and in vivo. Basic Res Cardiol 2005;100:397–403.
9. Hannon JP, Tigani B, Wolber C, et al. Evidence for an atypical receptor mediating the augmented bronchoconstrictor response to adenosine induced by allergen challenge in activity sensitized Brown Norway rats. Br J Pharmacol 2002;135:685–96.
10. Kin H, Zatta AJ, Lofye MT, et al. Postconditioning reduces infarct size via adenosine receptor activation by endogenous adenosine. Cardiovasc Res 2005;67:124–33.
11. Hinschen AK, RoseMeyer RB, Headrick JP. Adenosine receptor subtypes mediating coronary vasodilation in rat hearts. J Cardiovasc Pharmacol 2003;41:73–80.
12. Kaeffeer N, Richard V, Francois A, Lallemand F, Henry JP, Thuillez C. Preconditioning prevents chronic reperfusion-induced coronary endothelial dysfunction in rats. Am J Physiol 1996;271:H842–9.
13. M Shimizu, Miwa K, Hashimoto Y, Goto A. Encapsulating of chicken egg yolk immunoglobulin G (IgY) by liposomes. Biosci Biotechnol Biochem 1993;57:1445–9.
14. Kasuya T, Jung J, Kadoya H, et al. In vivo delivery of bionanocapsules displaying phaseolus vulgaris agglutinin-L(4) isolectin to malignant tumors overexpressing N-acetylglucosaminlyltransferase V. Hum Gene Ther 2008;19:887–95.
15. Kim YD, Fomsgaard JS, Heim KF, et al. Brief ischemia-reperfusion induces stunning of endothelium in canine coronary artery. Circulation 1992;85:1473–82.
16. Canyon SJ, Dobson GP. Protection against ventricular arrhythmias and cardiac death using adenosine and lidocaine during regional ischemia in the in vivo rat. Am J Physiol Heart Circ Physiol 2004;287:H1286–95.
17. Yaar R, Jones MR, Chen JF, Ravid K. Animal models for the study of adenosineÅreceptor function. J Cell Physiol 2005;202:9–20.
18. Norton ED, Jackson EK, Turner MB, Virmani R, Forman MB. The effects of intravenous infusions of selective adenosine A_1-receptor and A_2-receptor agonists on myocardial reperfusion injury. Am Heart J 1992;123:332–8.
19. Xu Z, Mueller RA, Park SS, Boysen PG, Cohen MV, Downey JM. Cardioprotection with adenosine A_2 receptor activation at reperfusion. J Cardiovasc Pharmacol 2005;46:794–802.
20. Vinten-Johansen J. Postconditioning: a mechanical maneuver that triggers biological and molecular cardioprotective responses to reperfusion. Heart Fail Rev 2007;12:235–344.
21. Lasic DD. Doxorubicin in sterically stabilized liposomes. Nature 1996;380:561–2.

Key Words: myocardial infarction ▪ liposome ▪ drug delivery system ▪ adenosine.

BRAIN RESEARCH XX (2010) XXX–XXX

available at www.sciencedirect.com

ScienceDirect

www.elsevier.com/locate/brainres

BRAIN RESEARCH

Research Report

Accumulation of macromolecules in brain parenchyma in acute phase of cerebral infarction/reperfusion

*Takayuki Ishii, Tomohiro Asai, Takeo Urakami, Naoto Oku**

Department of Medical Biochemistry and Global COE, School of Pharmaceutical Sciences, University of Shizuoka, 52-1 Yada, Suruga-ku, Shizuoka 422-8526, Japan

ARTICLE INFO

Article history:
Accepted 13 January 2010

Keywords:
Stroke
Reperfusion injury
BBB
t-MCAO
Macromolecule

ABSTRACT

Ischemia–reperfusion injury is induced by recovery of blood flow after ischemia. This phenomenon is a main cause of ischemic brain injury. The integrity of the blood–brain barrier (BBB) fails after cerebral ischemia and reperfusion. Further elucidation of this phenomenon promotes to develop treatment strategies for ischemia–reperfusion injury. In the present study, we attempted to examine the time-dependent change of ischemia–reperfusion injury in relation to BBB disorders at acute phase in a transient middle cerebral artery occlusion (t-MCAO) model rat as a cerebral infarction and reperfusion model. Brain cell damage after the reperfusion was assessed by 2, 3, 5-triphenyltetrazolium chloride (TTC) staining. To clarify a time-dependent change of the integrity of BBB, fluorescein isothiocyanate (FITC)-dextran (150 kDa) was injected intravenously into t-MCAO rats, and time-dependent localization of FITC-dextran was monitored in ex vivo. As a result, obvious brain damage was firstly observed at 3 h after reperfusion following 1 h of MCAO. In contrast, the leakage of FITC-dextran from cerebral vessels was observed immediately after the reperfusion. The present data suggest that the integrity of BBB failed prior to the occurrence of serious brain damage induced by ischemia–reperfusion, and that macromolecules such as water-soluble polymers and proteins which cannot pass through the BBB under normal condition would reach brain parenchyma at early stage after reperfusion. These findings would be useful to establish a novel treatment strategy for reperfusion injury after cerebral infarction.

1. Introduction

The BBB strictly limits material exchange in the brain, which makes drug delivery to the brain tissue difficult. However, it is known that the integrity of the BBB fails after cerebral ischemia and reperfusion, resulting in increase in cerebrovascular permeability (Yang and Betz, 1994). Several factors including reactive oxygen species, matrix metalloprotease (MMP)-2, and -9, vascular endothelial growth factor (VEGF) are considered to be related with increase in permeability by change of cerebral vascular tonus and disruption of basement membrane after reperfusion following cerebral stroke (Rosenberg et al., 1998; Zhang et al., 2002).

In the treatment of cerebral stroke, ischemic penumbra is one of the most important concepts (Lo, 2008). It is defined as ischemic but still viable cerebral tissue. This area recovers if cerebral blood flow is rapidly improved. The aim of treatment for acute phase of cerebral stroke is to recover cerebral blood

* *Corresponding author.* Fax: +81 54 264 5705.
E-mail address: oku@u-shizuoka-ken.ac.jp (N. Oku).

0006-8993/$ – see front matter © 2010 Elsevier B.V. All rights reserved.
doi:10.1016/j.brainres.2010.01.039

Please cite this article as: Ishii, T., et al., Accumulation of macromolecules in brain parenchyma in acute phase of cerebral infarction/reperfusion, Brain Res. (2010), doi:10.1016/j.brainres.2010.01.039

flow and to revive the function of neuronal cells in the penumbra. However, many deleterious mediators are upregulated and injure brain tissue by reperfusion after ischemia. For example, reactive oxygen species such as hydrogen peroxide, hydroxyl radicals and superoxide are produced by reperfusion following brain ischemia (Kontos, 2001). They cause cerebral vasodilatation, resulting in brain tissue injury. In fact, α-amino-3-hydroxy-5-methylisoxasolepropionic acid (AMPA) is known to mediate superoxide generation, and the inhibition of AMPA receptor improves ischemic outcome (Erdo et al., 2005). Many other pathways are also involved in secondary brain lesion after cerebral infarction (Cunningham et al., 2005; Huang et al., 2006). This cerebral ischemia–reperfusion injury substantially influences prognosis and mortality of patients treated with thrombolytic agents for cerebral infarct therapy. Therefore, improvement of ischemia–reperfusion injury is essential for the treatment of cerebral ischemia and required to protect a cerebral neuronal cell. Although mechanisms of reperfusion injury after cerebral infarction have been widely studied in the world, clinically available drug at present is only Radicut® (edaravone), a free radical scavenger, for cerebral neuroprotection during cerebral ischemia/reperfusion (Yoshida et al., 2006).

In the case of acute disease such as cerebral infarction, therapeutic time window (TTW) is an important concept. It is defined as the promising time to achieve therapeutic efficacy. For example, tissue plasminogen activator (t-PA), a thrombolytic agent, for treatment of cerebral stroke is decided to inject within 3 h because it has prospects of worsening symptoms more than 3 h after ischemia (Marler and Goldstein, 2003).

t-MCAO model rats by a filament method are used to the study of ischemia–reperfusion injury after focal ischemia (Nagasawa and Kogure, 1989). This method can make a stable cerebral occlusion model using a nylon uniformly coated with silicon. In addition, reperfusion is induced easily by pulling the thread out of the artery. Since this model needs no materials such as t-PA to induce reperfusion, the influences of reperfusion can be observed directly without considering superfluous factors.

Macromolecules with biocompatibility and size above 40 kDa possess long-circulating characteristic in bloodstream, and tend to localize at the site where the vascular permeability is increased (Seymour et al., 1995). In fact, vascular permeability is known to increase at inflammatory site, and a dendritic polymer complexed with ibuprofen is reported to localized and retained at the inflammatory site resulting in a high anti-inflammatory effect (Kannan et al., 2004; Svenson, 2009). Moreover, in myocardial ischemia/reperfusion that shows similar pathological event to cerebral ischemia/reperfusion, macromolecular agents accumulated in the infarction zone at early stage by vascular permeability increase (Lukyanov et al., 2004). However it isn't known that time-dependent change in the extent of diffusion of macromolecules into brain tissue by disruption of the BBB after cerebral ischemia/reperfusion in acute phase.

In the present study, we attempted to clarify the time-dependent relationship between ischemia–reperfusion damage and localization of macromolecules by increasing BBB permeability in t-MCAO model rats for the purpose of the determination of effective term for the treatment of reperfusion injury using macromolecular drugs or drugs in macromolecules.

2. Results

2.1. *Brain damage assessment*

The time-dependent change of ischemia/reperfusion damage was assessed by TTC staining. A ratio between right and left hemisphere section areas represents brain edema. When this ratio significantly exceeds 1, edema is induced on the side of the occlusion. Fig. 1 shows representative photographs of the brain damage in the t-MCAO rats. Total brain slice areas and damaged ones are calculated by Image J, and their mean values are shown in Table 1. The damage of the brain tissue was firstly observed in the section of the MCA at 3 h after the reperfusion. At 6 h after the reperfusion, the damage was observed more broadly than at 3 h, and the cell death progressed to cerebral cortex. Moreover, the most widespread damage was observed at 24 h after the reperfusion. Similarly, the brain edema was firstly observed at 3 h after the reperfusion. However, significant cerebral damage was not observed until 3 h after the reperfusion.

2.2. *Leakage of FITC-dextran*

Time course of the change in cerebral blood vessel permeability after reperfusion in the t-MCAO rat were monitored by the leakage of FITC-dextran with in vivo imaging system. Fig. 2 shows the leakage of FITC-dextran into brain parenchyma at 1 h after the administration. Table 2 shows average of total photon counts obtained from five rats at each time. Interestingly, the leakage of the FITC-dextran from cerebral vessels was observed immediately after the reperfusion in the t-MCAO rat model. This leakage was observed up to 6 h but not at 24 h after the reperfusion. The FITC-dextran localization in brain tissue became broadly as time advances within 3 h. However, the fluorescence intensity was diminished at 6 h compared with that at 3 h.

In the present study, we did not use the same slices in both TTC staining and FITC imaging due to the technical limitation. However the slices were obtained essentially by the same procedure except the injection of FITC-dextran in the latter experiment. Therefore, both TTC staining and FITC imaging would be comparable.

3. Discussion

In the present study, the reperfusion was performed by withdrawing the filament at 1 h after the occlusion using t-MCAO model rats. Although nerve cells suspend electrical activity under ischemic condition, their life is maintained for a few hours because of conservation of ion gradient and cellular membrane pump function (Back, 1998). Therefore, the damage observed in the present study could be mainly derived from reperfusion. Taken together, most of the penumbra area might be protected from death by restoration of blood flow if a treatment for neuroprotection is performed within therapeutic time window.

Cells death of the core infarct area arises predominantly from necrosis, whereas cell death of penumbra area is caused

Please cite this article as: Ishii, T., et al., Accumulation of macromolecules in brain parenchyma in acute phase of cerebral infarction/reperfusion, Brain Res. (2010), doi:10.1016/j.brainres.2010.01.039

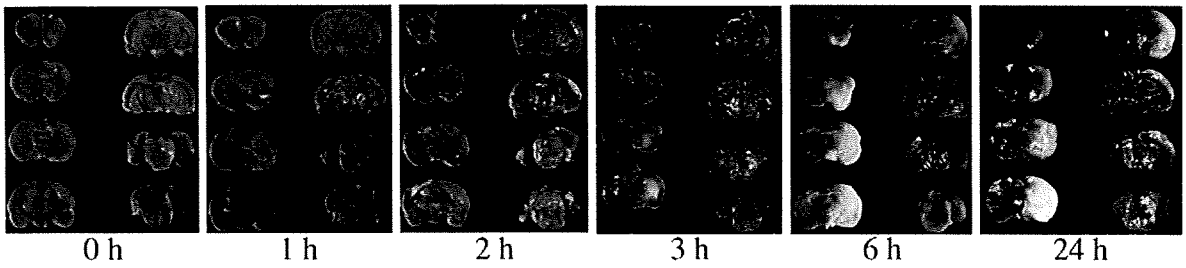

Fig. 1 – Photographs of brain sections prepared from the t-MCAO model rats. The damaged regions were visualized by TTC staining after a 1 h-infarct following 0, 1, 2, 3, 6 or 24 h reperfusion. White areas show the damaged regions and red areas show surviving regions.

mainly by apoptosis following cerebral ischemia (Dirnagl et al., 1999; Lopez-Sanchez et al., 2007; Xu et al., 2006). Therefore, an antiapoptotic agent would protect neuronal cells and attenuate reperfusion injury. In fact, pretreated inhibition of caspase-3 results in decrease of cerebral damage in the penumbra area following 2 h infarct (Zhu et al., 2004). Apoptosis is a key factor improving reperfusion injury, and the detail researches contribute to a new treatment strategy for ischemia–reperfusion injury.

The BBB dysfunction results in cerebral edema, hemorrhage formation and neuronal cell death after cerebral infarction. On the other hand, it permits some drugs that cannot penetrate the BBB in normal condition to reach brain parenchyma. Therefore, it would be one of the promising strategies for improving ischemia–reperfusion injury to delivery agents to brain tissue from cerebral blood flow by increasing BBB permeability. Opening of the BBB has been studied by using many tracers in ischemia/reperfusion. After 2 h occlusion and 3 h reperfusion caused great increase in BBB permeability, which was monitored by the uptake of sucrose (Rosenberg et al., 1998). In the present study, we determined the leakage of macromolecule in more acute phase ischemia/reperfusion. The leakage of FITC-dextran into brain tissue was observed just after the reperfusion in the t-MCAO rat model. These data suggest that tight junction of the BBB fails by reperfusion or 1 h infarct and thus macromolecules such as dextran leak out from bloodstream into the brain tissue. Our findings are consistent with previous reports: For example, a function of myogenic tone, which favors partial vasoconstriction and plays an important role in regulation of cerebrovascular blood flow in response to changes in perfusion pressure, was diminished at early stage after ischemia (Cipolla et al., 1997; Cipolla and Curry, 2002). MMP-2 derived from astrocyte increases at 3 h after reperfusion in the same model rat as the present study (Yang et al., 2007). Therefore, this data suggest that upregulation of MMP-2 is greatly associated with the present result that leakage of FITC-dextran was most broadly at 3 h after reperfusion. Hydroxyl radicals that are one of the most reactivity free radicals greatly increase at immediately after reperfusion in the same model rat as the present study (Kato et al., 2003). Free radicals are related with BBB disruption on how to directly attack cerebral endothelial cells and to mediate MMPs. This report is also associated with the result in the present study. Focusing on the result of 0, 1 and 3 h after reperfusion, fluorescence of FITC-dextran was observed at nearby MCA. In addition, the leakage of FITC-dextran was outspread as time advances. Therefore, BBB disruption progress gradually with time by partial infarct, in this study case is by MCA, after reperfusion.

When neuroprotective agents are delivered to brain tissue for the treatment of ischemia–reperfusion injury by enhanced permeability of a failed BBB, a time widow from appearance of BBB disruption to disappearance of it is very important notion. The integrated data demonstrated that the increase of cerebral vascular permeability from BBB dysfunction was occurred at stages before generation of obvious cerebral cell damage in the t-MCAO model rats. This is important information for the treatment and prevention of reperfusion injury. In general, therapeutic agents for acute phase treatment are beneficial as early injection as possible. However, it is also quite important to know until when do these agents are effective after ischemia–reperfusion. For this reason, here we evaluated the permeability change in BBB and brain damage after ischemia–reperfusion to set TTW in acute phase disease. From the present results, we propose that TTW of reperfusion injury is from immediately after reperfusion up to 3 h. At 6 h after the reperfusion, the brain tissue was broadly impaired, and the leakage of FITC-dextran was diminished, hence suggesting that the possibility to save brain cells is lowered. Obvious cerebral cell death was rarely observed up to 3 h after the reperfusion, and the localization of FITC-dextran was observed earlier than outset of the obvious cerebral cell death. Therefore, some treatments before 3 h after reperfusion are

Table 1 – Time-dependent change of brain injury.

Times after reperfusion	Total volume (cm^3)	Damage volume (cm^3)	Right brain/ left brain
0 h	1.60±0.02	0	1.00±0.00
1 h	1.61±0.02	0	1.01±0.01
2 h	1.61±0.07	0	1.01±0.01
3 h	1.70±0.03	0.05±0.06	1.04±0.02*
6 h	1.72±0.06	0.27±0.07	1.06±0.01**
24 h	1.81±0.05	0.42±0.03	1.12±0.04**

Values are means±SD; $n=5$. Right brain/left brain shows the degree of edema. Statistical differences were calculated by one-way analysis of variance (ANOVA) followed by Dunnett's multiple comparison tests as compared with 0 h after reperfusion group. (*$p<0.05$, **$p<0.01$).

Please cite this article as: Ishii, T., et al., Accumulation of macromolecules in brain parenchyma in acute phase of cerebral infarction/reperfusion, Brain Res. (2010), doi:10.1016/j.brainres.2010.01.039

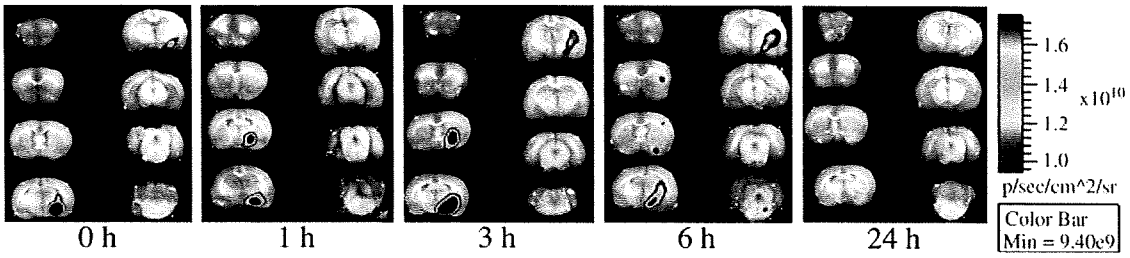

Fig. 2 – The leakage of FITC-dextran in the t-MCAO model rats. Time-dependent change in the integrity of BBB after the reperfusion was monitored by the leakage of FITC-dextran. The t-MCAO rats were injected with FITC-dextran solution (15 mg/ rat i.v.). FITC-dextran localized in the brain sections was visualized with IVIS. Bar shows the relative level of fluorescence intensity, ranging from low (blue), to medium (green), to high (yellow, red). This is the representative from five independent animal experiments, all of which demonstrated similar profile of responses. (For interpretation of the references to color in this figure legend, the reader is referred to the web version of this article.)

expected to be significantly effective for the improvement in reperfusion injury.

In conclusion, macromolecules leaked out from blood-stream into brain parenchyma before the obvious cerebral cell death appeared in t-MCAO model rats, and this localization was broadly more than the damage area at 3 h after the reperfusion. The present study suggests that an approach within 3 h after reperfusion is important and promising for the treatment or prevention of reperfusion injury to provide great therapeutic response.

4. Experimental procedures

4.1. *Animal*

Male Wistar rats (8 weeks old) weighing 170–210 g were purchased from Japan SLC Inc. (Shizuoka, Japan). The animals were cared according to the Animal Facility Guidelines of the University of Shizuoka. All animal experiments were approved the by the Animal and Ethics Review Committee of the University of Shizuoka.

4.2. *Preparation of t-MCAO model rat*

Transient middle cerebral artery occlusion (t-MCAO) was induced by inserting a filament into internal carotid artery (Nagasawa and Kogure, 1989). Anesthesia was induced with 3% isoflurane and maintained with 1.5% one during cerebral stroke surgery. Rectal temperature was maintained at 37 °C with heating pad. After a median incision of the neck skin, the right carotid artery, external carotid artery, and internal carotid artery (ICA) were isolated with careful conservation of the vagal nerve. A 4-0 monofilament nylon suture coated with silicon was introduced into the right ICA and advanced into the origin of the MCA. A silk ligated the MCA at side of inserting point. After the operation, the neck was closed and anesthesia was discontinued. Success of the surgery was judged by the appearance of hemiparesis. Reperfusion was performed by withdrawing the filament about 10 mm at 1 h after the occlusion under isoflurane anesthesia in this all study.

Table 2 – Total photon counts of brain sections.

Injection time	Ischemic side ($\times 10^7$)	Nonischemic side ($\times 10^7$)
0 h	4.18±0.32*	3.58±0.16
1 h	5.71±1.28*	3.64±0.69
3 h	6.70±2.47*	3.83±0.57
6 h	4.21±1.11	3.37±0.59
24 h	4.09±0.67	3.83±0.38

Values are means±SD; $n=5$. Accumulation of FITC-dextran in the brain was determined as described in the legend of Fig. 2. Total photon counts were obtained from the IVIS images. Total photon counts of ischemic side are significantly higher than those of nonischemic side at 0, 1 and 3 h. (*$p<0.05$).

4.3. *Brain damage assessment in t-MCAO rat*

The ischemia/reperfusion damage in the t-MCAO rat model was assessed by morphometric analysis of the brain sections stained with 2, 3, 5-triphenyltetrazolium chloride (TTC, Wako Pure Chemical Ind. Ltd., Tokyo, Japan). The brain was dissected at 0, 1, 2, 3, 6 or 24 h after reperfusion and sliced into 2 mm thick coronal sections using a rat brain slicer (Muromachi Kikai, Tokyo, Japan). These sections were stained with 2% TTC in PBS for 30 min at 37 °C. Then, they were fixed in 10% formalin neutral buffer solution. All sections were put in grass slides and photographed with a digital camera (OLYMPUS E-300). We measured the unstained area, the stained area and each hemisphere with an image analysis system (NIH Image J). The damage regions were considered as completely white area. Edema was calculated from a ratio between right and left hemisphere sections area.

4.4. *Leakage of FITC-dextran into brain tissue*

Time-dependent change of the integrity of BBB after reperfusion was determined using fluorescein isothiocyanate (FITC)-dextran (150 kDa, Sigma-Aldrich, Saint Louis, MO, USA) as a macromolecule. FITC-dextran (0.5 mL) dissolved in saline (30 mg/mL) was injected via a tail vain of the t-MCAO rat model at 0, 1, 3, 6 or 24 h after reperfusion, respectively. One

Please cite this article as: Ishii, T., et al., Accumulation of macromolecules in brain parenchyma in acute phase of cerebral infarction/reperfusion, Brain Res. (2010), doi:10.1016/j.brainres.2010.01.039

hour after the injection, the brain was dissected and sliced into 2 mm thick coronal sections in the exactly same way as above experiment. All sections were put in grass slides and their fluorescence was measured at with in vivo imaging system (IVIS, Xenogen Corp., Alameda, CA).

REFERENCES

Back, T., 1998. Pathophysiology of the ischemic penumbra—revision of a concept. Cell. Mol. Neurobiol. 18, 621–638.

Cipolla, M.J., McCall, A.L., Lessov, N., Porter, J.M., 1997. Reperfusion decreases myogenic reactivity and alters middle cerebral artery function after focal cerebral ischemia in rats. Stroke 28, 176–180.

Cipolla, M.J., Curry, A.B., 2002. Middle cerebral artery function after stroke: the threshold duration of reperfusion for myogenic activity. Stroke 33, 2094–2099.

Cunningham, L.A., Wetzel, M., Rosenberg, G.A., 2005. Multiple roles for MMPs and TIMPs in cerebral ischemia. Glia 50, 329–339.

Dirnagl, U., Iadecola, C., Moskowitz, M.A., 1999. Pathobiology of ischaemic stroke: an integrated view. Trends Neurosci. 22, 391–397.

Erdo, F., Berzsenyi, P., Andrasi, F., 2005. The AMPA-antagonist talampanel is neuroprotective in rodent models of focal cerebral ischemia. Brain Res. Bull. 66, 43–49.

Huang, J., Upadhyay, U.M., Tamargo, R.J., 2006. Inflammation in stroke and focal cerebral ischemia. Surg. Neurol. 66, 232–245.

Kannan, S., Kolhe, P., Raykova, V., Glibatec, M., Kannan, R.M., Lieh-Lai, M., Bassett, D., 2004. Dynamics of cellular entry and drug delivery by dendritic polymers into human lung epithelial carcinoma cells. J. Biomater. Sci. Polym. Ed. 15, 311–330.

Kato, N., Yanaka, K., Hyodo, K., Homma, K., Nagase, S., Nose, T., 2003. Stable nitroxide Tempol ameliorates brain injury by inhibiting lipid peroxidation in a rat model of transient focal cerebral ischemia. Brain Res. 979, 188–193.

Kontos, H.A., 2001. Oxygen radicals in cerebral ischemia: the 2001 Willis lecture. Stroke 32, 2712–2716.

Lo, E.H., 2008. A new penumbra: transitioning from injury into repair after stroke. Nat. Med. 14, 497–500.

Lopez-Sanchez, C., Martin-Romero, F.J., Sun, F., Luis, L., Samhan-Arias, A.K., Garcia-Martinez, V., Gutierrez-Merino, C., 2007. Blood micromolar concentrations of kaempferol afford protection against ischemia/reperfusion-induced damage in rat brain. Brain Res. 1182, 123–137.

Lukyanov, A.N., Hartner, W.C., Torchilin, V.P., 2004. Increased accumulation of PEG-PE micelles in the area of experimental myocardial infarction in rabbits. J. Control. Release 94, 187–193.

Marler, J.R., Goldstein, L.B., 2003. Medicine. Stroke—tPA and the clinic. Science 301, 1677.

Nagasawa, H., Kogure, K., 1989. Correlation between cerebral blood flow and histologic changes in a new rat model of middle cerebral artery occlusion. Stroke 20, 1037–1043.

Rosenberg, G.A., Estrada, E.Y., Dencoff, J.E., 1998. Matrix metalloproteinases and TIMPs are associated with blood–brain barrier opening after reperfusion in rat brain. Stroke 29, 2189–2195.

Seymour, L.W., Miyamoto, Y., Maeda, H., Brereton, M., Strohalm, J., Ulbrich, K., Duncan, R., 1995. Influence of molecular weight on passive tumour accumulation of a soluble macromolecular drug carrier. Eur. J. Cancer. 31A, 766–770.

Svenson, S., 2009. Dendrimers as versatile platform in drug delivery applications. Eur. J. Pharm. Biopharm. 71, 445–462.

Xu, X.H., Zhang, S.M., Yan, W.M., Li, X.R., Zhang, H.Y., Zheng, X.X., 2006. Development of cerebral infarction, apoptotic cell death and expression of X-chromosome-linked inhibitor of apoptosis protein following focal cerebral ischemia in rats. Life Sci. 78, 704–712.

Yang, G.Y., Betz, A.L., 1994. Reperfusion-induced injury to the blood-brain barrier after middle cerebral artery occlusion in rats. Stroke 25, 1658–1664 discussion 1664-5.

Yang, Y., Estrada, E.Y., Thompson, J.F., Liu, W., Rosenberg, G.A., 2007. Matrix metalloproteinase-mediated disruption of tight junction proteins in cerebral vessels is reversed by synthetic matrix metalloproteinase inhibitor in focal ischemia in rat. J. Cereb. Blood Flow Metab. 27, 697–709.

Yoshida, H., Yanai, H., Namiki, Y., Fukatsu-Sasaki, K., Furutani, N., Tada, N., 2006. Neuroprotective effects of edaravone: a novel free radical scavenger in cerebrovascular injury. CNS Drug Rev. 12, 9–20.

Zhang, Z.G., Zhang, L., Tsang, W., Soltanian-Zadeh, H., Morris, D., Zhang, R., Goussev, A., Powers, C., Yeich, T., Chopp, M., 2002. Correlation of VEGF and angiopoietin expression with disruption of blood–brain barrier and angiogenesis after focal cerebral ischemia. J. Cereb. Blood Flow Metab. 22, 379–392.

Zhu, H.C., Gao, X.Q., Xing, Y., Sun, S.G., Li, H.G., Wang, Y.F., 2004. Inhibition of caspase-3 activation and apoptosis is involved in 3-nitropropionic acid-induced ischemic tolerance to transient focal cerebral ischemia in rats. J. Mol. Neurosci. 24, 299–305.

Please cite this article as: Ishii, T., et al., Accumulation of macromolecules in brain parenchyma in acute phase of cerebral infarction/reperfusion, Brain Res. (2010), doi:10.1016/j.brainres.2010.01.039

Cancer Letters 287 (2010) 165–171

Contents lists available at ScienceDirect

Cancer Letters

journal homepage: www.elsevier.com/locate/canlet

A novel DDS strategy, "dual-targeting", and its application for antineovascular therapy

Yuki Murase [a], Tomohiro Asai [a], Yasufumi Katanasaka [a], Tomoki Sugiyama [a], Kosuke Shimizu [a], Noriyuki Maeda [b], Naoto Oku [a,*]

[a] Department of Medical Biochemistry and Global COE Program, Graduate School of Pharmaceutical Sciences, University of Shizuoka, 52-1 Yada, Suruga-ku, Shizuoka 422-8526, Japan
[b] Nippon Fine Chemical Co. Ltd., Takasago, Hyogo 676-0074, Japan

ARTICLE INFO

Article history:
Received 16 December 2008
Received in revised form 25 March 2009
Accepted 8 June 2009

Keywords:
Dual-targeting
Drug delivery system
Liposomes
Active-targeting
Antineovascular therapy
Angiogenesis

ABSTRACT

Dual-targeting liposomes modified with Ala-Pro-Arg-Pro-Gly (APRPG) and Gly-Asn-Gly-Arg-Gly (GNGRG) peptides were developed. They remarkably associated to growing human umbilical vein endothelial cells (HUVECs) compared with single-targeting liposomes modified with APRPG or GNGRG. Doxorubicin (DOX) encapsulated in the dual-targeting liposomes significantly suppressed the growth of HUVECs compared with that in single-targeting liposomes. The dual-targeting liposomes containing DOX strongly suppressed tumor growth in Colon26 NL-17 carcinoma-bearing mice. Confocal microscopic data indicated that this anticancer effect was brought by the association of these liposomes to angiogenic vessels in the tumor. These findings suggest that "dual-targeting" would be a hopeful method for targeting therapies.

1. Introduction

Liposomes are known as one of the most effective drug carriers for cancer therapy. In liposomal DDS technologies, polyethylene glycol (PEG)-modified liposomes are well known as useful drug carriers for cancer therapy. PEG-modified liposomes have long-circulating characteristics through avoidance of trapping by a reticuloendothelial system (RES) such as liver and spleen [1,2]. PEG-modified liposomes tend to accumulate in tumor tissues thorough passive targeting since leaky angiogenic vessels brings enhanced permeability and retention (EPR) effect [3,4]. In fact, PEG-modified liposomes containing doxorubicin (DOX) have been used in clinical cancer therapy. On the other hand, active-targeting using liposomes modified with ligands such as antibodies and peptides achieves more selective drug delivery to tumor tissues. These ligands that recognize tumor-associated molecules are conjugated to the head of PEG-chain of liposomes [5,6]. Active-targeting using ligand-modified long-circulating PEG-liposomes would be more effective since these liposomes have great opportunity to meet target tissues during long circulation time. Indeed, cancer treatments with stealth immunoliposomes and transferrin-conjugated PEG-liposomes have been successful in animal models [7–9].

Abbreviations: DDS, drug delivery system; APRPG, Ala-Pro-Arg-Pro-Gly; GNGRG, Gly-Asn-Gly-Arg-Gly; ANET, antineovascular therapy; HUVECs, human umbilical vein endothelial cells; DOX, doxorubicin; PEG, polyethylene glycol; RES, reticuloendothelial system; EPR, enhanced permeability and retention; RGD, Arg-Gly-Asp; DSPC, distearoylphosphatidylcholine; EGM-2, endothelial cell growth medium-2; FBS, fetal bovine serum; ANOVA, analysis of variance; PEG-Lip, PEG-modified liposomes; PRP-PEG-Lip, APRPG-modified liposomes; NGR-PEG-Lip, GNGRG-modified liposomes; Dual-PEG-Lip, dual-targeting liposomes; PEG-DOX, DOX encapsulated in PEG-Lip; PRP-PEG-DOX, DOX encapsulated in PRP-PEG-Lip; NGR-PEG-DOX, DOX encapsulated in NGR-PEG-Lip; Dual-PEG-DOX, DOX encapsulated in Dual-PEG-Lip; EGFR, epidermal growth factor receptors; FR, folate receptors.

* Corresponding author. Tel.: +81 54 264 5701; fax: +81 54 264 5705.
E-mail address: oku@u-shizuoka-ken.ac.jp (N. Oku).

0304-3835/$ - see front matter © 2009 Elsevier Ireland Ltd. All rights reserved.
doi:10.1016/j.canlet.2009.06.008

Angiogenesis is a critical event for growth and hematogenous metastasis of tumors [10,11]. Therefore, antiangiogenic therapies are promised to suppress both tumor growth and metastasis [12,13]. Antineovascular therapy (ANET), one of antiangiogenic therapies, causes indirect tumor regression through damaging angiogenic vessels, which is achieved by delivering anticancer drugs to them with DDS technologies such as liposomes [14]. ANET could avoid the acquirement of drug resistance resulting from genetic or epigenetic mutation since this therapy targets angiogenic endothelial cells that are genetically stable [13]. The therapeutic effect of anticancer drugs would be amplified by targeting angiogenic cells since a large number of cancer cells are maintained by a relatively few endothelial cells for their survival and growth [15]. Furthermore, ANET is expected to have a broad anticancer spectrum since angiogenic vessels are necessary for all kinds of solid tumors.

We previously performed *in vivo* biopanning of a phage-displayed peptide library using an angiogenesis mouse model to identify a targeting-ligand for angiogenic vessel-specific drug delivery. As a result, Ala-Pro-Arg-Pro-Gly (APRPG) was identified as a novel peptide homing to angiogenic vessels [14,16]. Arap and coworkers injected phage-displayed peptide library into the circulation of human breast carcinoma-bearing mice and identified Asn-Gly-Arg (NGR) and Arg-Gly-Asp (RGD) motif [17]. NGR and RGD peptides motif bind selectively to CD13 (aminopeptidase N) and $\alpha_v\beta_3$ or $\alpha_v\beta_5$ integrins, respectively [18–20]. These peptides such as PRP, NGR and RGD were useful as targeting-ligands of liposomes since modification of liposomes with each of these peptides enhanced anticancer activity of DOX in tumor-bearing mice [21,22]. Until now, these peptides were used for angiogenic vessel-targeting individually and combinational effect of them has not been investigated. In the present study, we proposed a novel active-targeting strategy named "dual-targeting" in which two different kinds of targeting-ligands are modified on drug carriers. We hypothesized that two different ligands on the surface of liposomes might enable to enhance the potential of active-targeting cooperatively. We prepared dual-targeting liposomes modified with both APRPG and GNGRG and investigated the usefulness of them for ANET.

2. Materials and methods

2.1. Preparation of liposomes

All lipids were the products of Nippon Fine Chemical, Co. Ltd. (Takasago, Hyogo, Japan). Distearoylphosphatidylcholine (DSPC) and cholesterol with DSPE-PEG, DSPE-PEG-APRPG or DSPE-PEG-GNGRG (10:5:1 as a molar ratio), or with DSPE-PEG-APRPG and DSPE-PEG-GNGRG (10:5:0.5:0.5 as a molar ratio) were dissolved in chloroform/methanol, dried under reduced pressure, and stored *in vacuo* for at least 1 h. Liposomes were prepared by hydration of the thin lipid film with PBS, and frozen and thawed for three cycles using liquid nitrogen. Then, the liposomes were sized by extruding thrice through a polycarbonate membrane filter with 100 nm pores. Particle size and ζ-potential of the liposomes diluted with PBS were measured by use of a Zetasizer Nano ZS (MALVERN, Worcestershire UK, USA).

For an association study and a histochemical analysis, $DiIC_{18}$ (Molecular Probes Inc., Eugene, OR, USA) was added to the initial chloroform/methanol solution at a dose of 5 mol% of DSPC. For a biodistribution study, a trace amount of [^{3}H]cholesteryl hexadecyl ether (GE Healthcare UK Ltd., Buckinghamshire, England) was added to the initial solution. For a cell proliferation assay and a therapeutic experiment, DOX-encapsulated liposomes were prepared by a modification of the remote-loading method as described previously [23]. The encapsulation efficiency of DOX into the liposomes was more than 90% throughout the experiment. The concentration of DOX was determined by an absorbance at 484 nm.

2.2. Association of liposomes to HUVECs

Human umbilical vein endothelial cells (HUVECs, 2×10^4 cells/well) were seeded on gelatin-coated 24-well plate and cultured in endothelial cell growth medium-2 (EGM-2, Cambrex Bio Science Walkersville, Walkersville, MD) for 48 h at 37 °C in a 5% CO_2 incubator. Then, $DiIC_{18}$-labeled liposomes were added (final 0.05 or 0.1 mM as DSPC concentration) and incubated for 4 h at 37 °C. After washing these cells with ice-cold PBS, they were solubilized in 0.1% sodiumdodecylsulfate-containing 10 mM Tris buffer (pH 7.4). The amount of $DiIC_{18}$-labeled liposomes transferred to HUVECs was fluorometrically determined at an excitation wavelength of 549 nm and an emission wavelength of 592 nm by Infinite M200 (Tecan, Grödig, Austria). The amount of proteins in the samples was determined by bicinchoninic acid (BCA) protein assay (Pierce Chemical, IL). The amount of liposomes transferred into HUVECs was corrected by the amount of cellular proteins.

2.3. Cell proliferation assay

HUVECs (5×10^3 cells/well) were seeded on gelatin-coated 96-well plate and cultured in EGM-2 overnight at 37 °C in a 5% CO_2 incubator. Then, DOX or DOX-encapsulated liposomes were added (final 10 μg/ml as a dose of DOX) and incubated for 30 min at 37 °C. After washing these cells with PBS, they were cultured in EGM-2 for 48 h. Then, the growth of these cells was evaluated by a modified MTT assay using TetraColor One™ (Seikagaku, Tokyo, Japan).

2.4. Biodistribution study

Colon26 NL-17 cells were cultured in DME/Ham's F12 medium (WAKO, Osaka, Japan) supplemented with streptomycin (100 μg/ml), penicillin (100 units/ml), and 10% fetal bovine serum (FBS) at 37 °C in 5% CO_2. After harvesting of these cells, 1.0×10^6 cells were implanted subcutaneously into the posterior flank of 4-week-old BALB/c male mice (Japan SLC Inc., Shizuoka, Japan). The biodistribution study was performed at day 11 after tumor implantation. Size-matched Colon26 NL-17-bearing mice ($n = 5$) were injected with the radiolabeled liposomes *via* a tail vein (74 kBq/mouse). Twenty-four hours after the injection, the mice

were sacrificed under deep anesthesia for collection of the blood. The plasma was obtained by centrifugation (600g for 5 min). Then the heart, lung, liver, spleen, kidney and tumor were removed, washed with saline, and weighed. The radioactivity in each organ was determined with a liquid scintillation counter (Aloka LSC-3100). Distribution data are presented as % dose per 100 mg tissue. The total amount in the plasma was calculated based on the body weight of mice, where the plasma volume was assumed to be 4.27% of the body weight based on the data of total blood volume [23]. The animals were cared for according to the animal facility guidelines of the University of Shizuoka.

2.5. Intratumoral localization of liposomes

Colon26 NL-17 cells (1.0×10^6 cells/mouse) were inoculated as described above. Dil-labeled liposomes were administered *via* a tail vein of the mice at 10 days after tumor implantation. At 3 h after injection of the liposomes, the mice were sacrificed under deep anesthesia, and the tumors were dissected. The tumor tissues were embedded in optimal cutting temperature compound (Sakura Finetech, Co. Ltd., Tokyo, Japan) and frozen at −80 °C. Tumor sections (10 μm) were prepared with cryostat microtome (HM 505E, Microm, Walldorf, Germany), mounted on MAS-coated slides (Matsunami Glass Ind., Ltd., Japan), air-dried for 1 h, and washed twice with PBS. Endogenous avidin activity was blocked with a blocking reagent kit (Vector Laboratories, CA). After these sections had been blocked with 1% BSA in PBS, they were incubated with biotinylated anti-mouse CD31 rat monoclonal antibody (Becton Dickinson Lab., Franklin Lakes, NJ) for 18 h at 4 °C and then visualized after incubation with streptavidin-Alexa fluor 488 conjugates (Molecular Probes Inc., Eugene, OR) for 30 min at room temperature in a humid chamber. Then, the sections were mounted with Perma Fluor Aqueous Mounting Medium (Thermo Shandon, PA) and fluorescently observed with the LSM 510 META confocal microscope (Carl Zeiss, Co. Ltd., Germany).

2.6. Therapeutic experiment

Colon26 NL-17 cells (1.0×10^6 cells/mouse) were inoculated as described above. DOX-encapsulated liposomes or PBS were administered intravenously into the tumor-bearing mice ($n = 5$) at day 8, 11, 14 and 17 after the tumor inoculation. The treatment was started when the tumor volumes had reached about 0.1 cm^3. The injected dose of DOX in each administration was 3 mg/kg (about 0.05 mmol/kg as a dose of DSPC in liposomal formulations). The size of the tumors and the body weight of each mouse were monitored. Two bisecting diameters of each tumor were measured with slide calipers to determine the tumor volume. Calculation of the tumor volume was performed using the formula $0.4 \times (a \times b^2)$, where a is the largest and b is the smallest diameter.

2.7. Statistical analysis

Differences in a group were evaluated by an analysis of variance (ANOVA) with the Tukey *post hoc* test.

3. Results

3.1. Characteristics of dual-targeting liposomes

Particle size and ζ-potential of liposomes were determined. All kinds of liposomes used in the following experiments had the size of 110–150 nm in diameter and slightly negative charges (Table 1).

3.2. Affinity of dual-targeting liposomes to proliferative endothelial cells

To investigate whether dual-targeting liposomes (Dual-PEG-Lip) have more potent affinity to angiogenic vessels compared with APRPG-PEG-modified or GNGRG-PEG-modified single-targeting liposomes (PRP-PEG-Lip or NGR-PEG-Lip), the association of dual-targeting liposomes to HUVECs stimulated with proangiogenic cytokines were determined (Fig. 1). As a result, all liposomes modified with targeting-peptides were significantly associated to HUVECs compared with PEG-modified liposomes (PEG-Lip) in a dose dependent manner. Moreover, the association amount of Dual-PEG-Lip to HUVECs was significantly higher than that of PRP-PEG-Lip and NGR-PEG-Lip.

3.3. Effect of DOX encapsulated in dual-targeting liposomes on the growth of HUVECs

Anti-proliferative effect of DOX encapsulated in dual-targeting liposomes (Dual-PEG-DOX) on HUVECs was determined (Fig. 2). DOX encapsulated in all targeting-liposomes tested (PRP-PEG-Lip containing DOX, PRP-PEG-DOX; NGR-PEG-Lip containing DOX, NGR-PEG-DOX; and Dual-

Table 1
Particle size and ζ-potential of liposomes.

	Particle size (nm)	ζ-Potential (mV)
PEG-Lip	121.6 ± 11.7	−3.1 ± 0.9
PRP-PEG-Lip	124.8 ± 21.4	−3.1 ± 0.6
NGR-PEG-Lip	122.7 ± 22.4	−2.3 ± 0.9
Dual-PEG-Lip	116.2 ± 9.7	−2.9 ± 0.8
PEG-DOX	145.7 ± 16.2	−1.2 ± 0.6
PRP-PEG-DOX	143.7 ± 28.4	−2.0 ± 0.3
NGR-PEG-DOX	145.0 ± 44.4	−2.0 ± 0.3
Dual-PEG-DOX	136.7 ± 34.0	−2.8 ± 1.6

Parameters represent the mean ± SD.

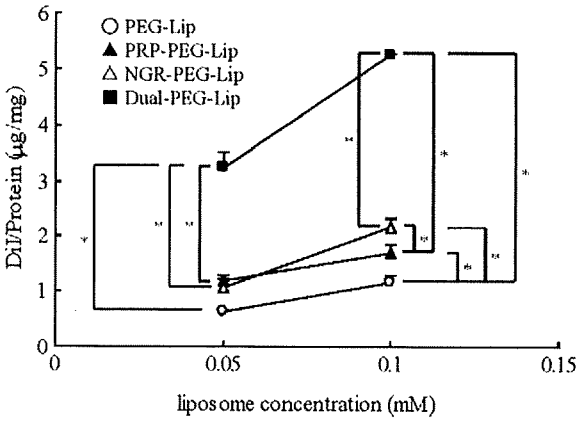

Fig. 1. The association of Dual-PEG-Lip to proliferating HUVECs. HUVECs were cultured in EGM-2 for 48 h, then added the indicated dose of $DiIC_{18}$-labeled liposomes and incubated for 4 h at 37 °C. After washing, the amount of liposomes associated to HUVECs was determined fluorometrically. Liposomes associated to HUVECs were represented as amount of $DiIC_{18}$ per cellular protein amount. Open circles, PEG-Lip; closed triangles, PRP-PEG-Lip; open triangles, NGR-PEG-Lip; and closed squares, Dual-PEG-Lip. Data show the mean value and SD. Significant differences are shown with asterisks ($^*P < 0.01$).

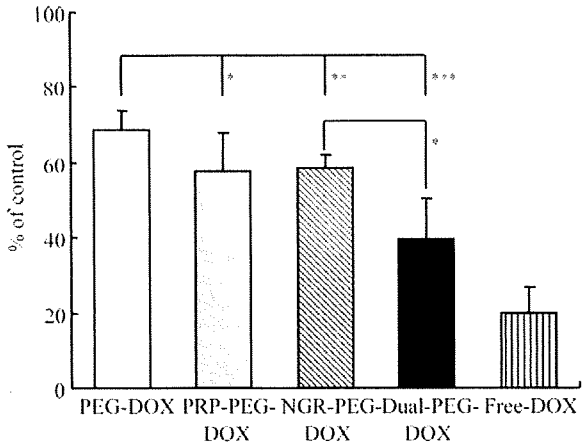

Fig. 2. Anti-proliferative effect of Dual-PEG-DOX on proliferating HUVECs. HUVECs were cultured in EGM-2 overnight. Then, DOX or DOX encapsulated in the liposomes were added (final concentration of 10 μg/ml as a DOX dosage) and incubated for 30 min at 37 °C. After 48 h incubation, cell growth was determined by modified MTT assay using TetraColor One™. Data represent the anti-proliferative effects of each sample as percent of control and SD. Open bar, PEG-DOX; grey bar, PRP-PEG-DOX; hatched bar, NGR-PEG-DOX; closed bar, Dual-PEG-DOX; and stripe bar, Free-DOX. Asterisks indicate the significant differences: $^{*}P < 0.05$, $^{**}P < 0.01$ and $^{***}P < 0.001$.

PEG-DOX) significantly suppressed the growth of HUVECs compared with DOX encapsulated in PEG-Lip (PEG-DOX). Furthermore, the antiproliferative effect of Dual-PEG-DOX was significantly higher than that of NGR-PEG-DOX and tended to be high compared with that of PRP-PEG-DOX. These anti-proliferative effects were observed in a dose dependent manner (Supplemental data).

3.4. Biodistribution of dual-targeting liposomes

The biodistribution of the liposomes was determined in Colon26 NL-17 carcinoma-bearing mice (Fig. 3). NGR-PEG-Lip tended to accumulate in the spleen. In contrast, the accumulation of PRP-PEG-Lip in the spleen

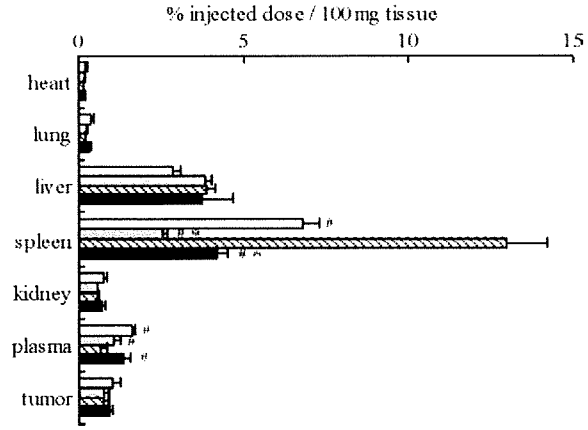

Fig. 3. Biodistribution of Dual-PEG-Lip in the tumor-bearing mice. Size-matched Colon26 NL-17-bearing mice ($n = 5$) were injected with radio-labeled liposomes *via* a tail vein. Twenty-four hours after injection, the radioactivity in each organ was determined. Data are presented as percent of the injected dose per 100 mg tissue and SD. Open bar, PEG-Lip; grey bar, PRP-PEG-Lip; hatched bar, NGR-PEG-Lip; and closed bar, Dual-PEG-Lip. Significant differences are shown with asterisks (versus PEG-Lip): $^{*}P < 0.01$, and sharps (versus NGR-PEG-Lip): $^{\#}P < 0.01$.

was lower than PEG-Lip. Interestingly, Dual-PEG-Lip did not accumulate in the spleen although it contains a half amount of GNGRG peptides in comparison to NGR-PEG-Lip. The amount of NGR-PEG-Lip in the plasma was significantly lower than other liposomes tested. On the other hand, Dual-PEG-Lip showed a long-circulating property like PEG-Lip and PRP-PEG-Lip. The accumulation in the tumor was similar level among all liposomes tested.

3.5. Intratumoral localization of dual-targeting liposomes

Intratumoral localization of the liposomes was determined in the tumor syngrafts to evaluate the affinity of Dual-PEG-Lip to angiogenic vessels *in vivo* (Fig. 4). As shown in Fig. 4a–c, PEG-Lip was observed around tumor angiogenic vessels, indicating that it extravasated from these vessels. On the other hand, PRP-PEG-Lip (Fig. 4d–f), NGR-PEG-Lip (Fig. 4g–i) and Dual-PEG-Lip (Fig. 4j–l) localized on angiogenic vessels. In addition, Dual-PEG-Lip localized on angiogenic vessels more intensely than PRP-PEG-Lip and NGR-PEG-Lip.

3.6. Therapeutic effect of DOX encapsulated in dual-targeting liposomes

The therapeutic effect of Dual-PEG-DOX against the solid tumor was examined (Fig. 5). The body weight change was not observed in all groups tested (data not shown). As shown in the figure, significant differences in the tumor volume were observed between liposomal DOX-treated group (PEG-DOX, PRP-PEG-DOX, NGR-PEG-DOX or Dual-PEG-DOX) and control group 24 days after tumor implantation. Antitumor effect of Dual-PEG-DOX was the highest among all liposomal formulations. Dual-PEG-DOX significantly suppressed the tumor growth in comparison to PEG-DOX.

4. Discussion

In the present study, we proposed a novel targeting strategy, "dual-targeting", and applied it to ANET. We firstly determined the affinity of liposomes modified with two different targeting peptides (namely APRPG and GNGRG) to proliferating HUVECs as an *in vitro* model of angiogenic endothelial cells. As a result, Dual-PEG-Lip showed the highest affinity to proliferating HUVECs dose-dependently. This data suggests that two different kinds of angiogenic vessel-targeting peptides on the liposomal surface cooperatively enhanced the association of these liposomes to proliferating HUVECs. Saul et al. previously reported that liposomes targeting epidermal growth factor receptors (EGFR) and folate receptors (FR) improved selectivity to target cells compared with single-ligand liposomes [24]. Although these liposomes attenuated non-specific binding to non-target cells, the affinity of them to target cells was not determined. In contrast, our data provided the evidence that dual-targeting achieved enhancement of the targeting activity. In fact, Dual-PEG-DOX suppressed the growth of proliferating HUVECs in comparison to non-targeting or single-targeting liposomal DOX, reflecting that Dual-PEG-Lip showed the highest affinity to proliferating HUVECs.

Previous study showed that liposomes modified with NGR accumulated in the spleen after intravenous injection [22]. Our data also indicated that NGR-PEG-Lip tended to accumulate in the spleen. However, this wrong property caused by NGR was improved in Dual-PEG-Lip administration group. Consequently, Dual-PEG-Lip remained in the plasma more than NGR-PEG-Lip. These results might be related to the amount of peptide on the liposome surface although precise mechanism is not cleared at present. There were no statistical differences in the accumulation

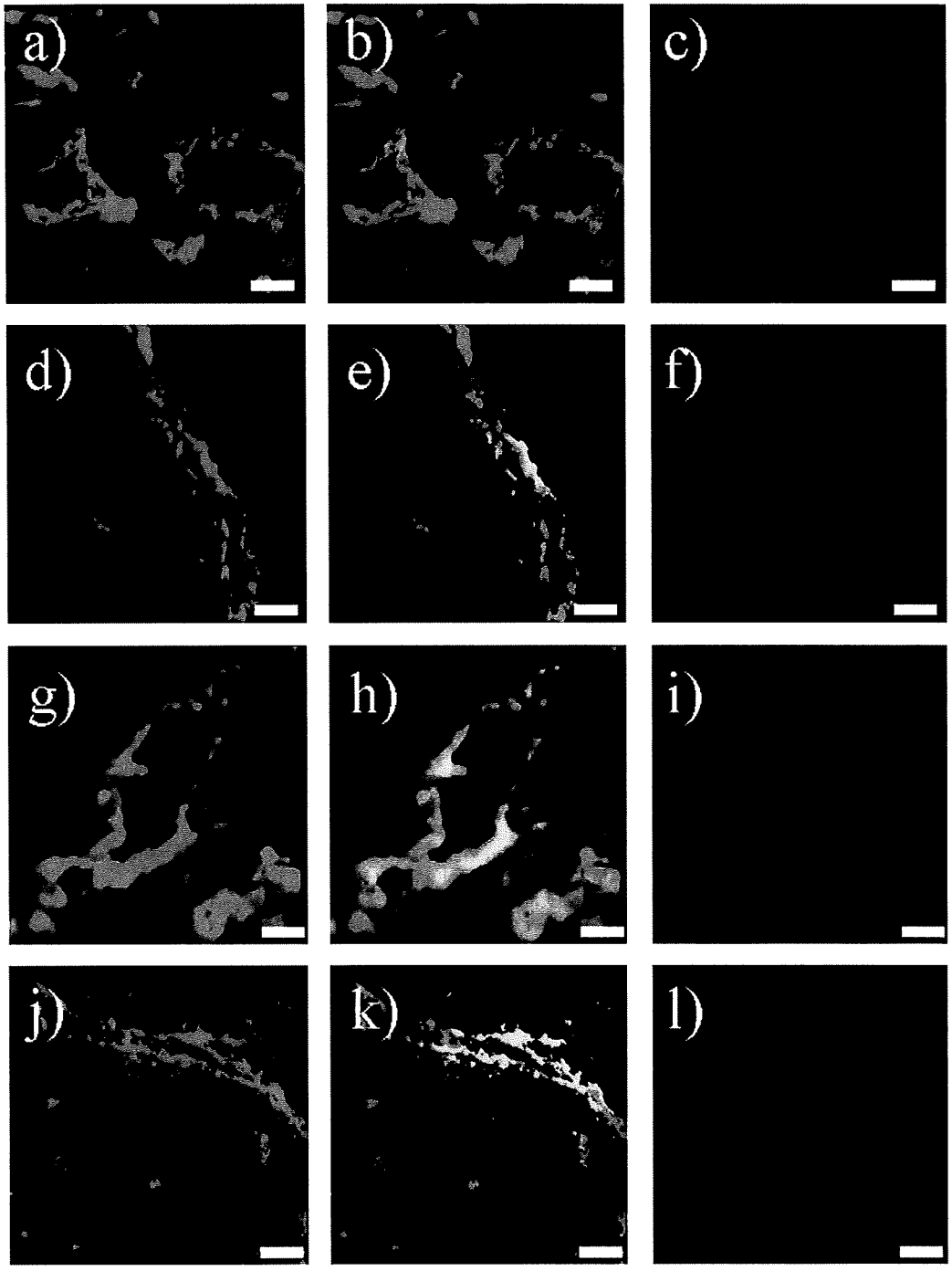

Fig. 4. Localization of Dual-PEG-Lip in the tumor. Colon26 NL-17-bearing mice were intravenously injected with PEG-Lip (a–c), PRP-PEG-Lip (d–f), NGR-PEG-Lip (g–i) or Dual-PEG-Lip (j–l) labeled with $DiIC_{18}$ at day 10 after tumor implantation. At 3 h after injection, the tumors were dissected, and then frozen-sections (10 μm) were prepared. Immunofluorescence staining for CD31 was performed to visualize endothelial cells. Green images indicate CD31-positive regions (a, d, g and j), and red images show liposomal distribution (c, f, i and l). Panels b, e, h and k represent the merged images of them. Yellow portions indicate the localization of liposomes at the site of vascular endothelial cells. Scale bars represent 20 μm.

of liposomes to tumor tissue. However, intratumoral distribution of Dual-PEG-Lip in Colon26 NL-17-bearing mice was obviously different. The results showed that targeting liposomes bound to angiogenic vessels whereas PEG-Lip did not. Moreover, Dual-PEG-Lip showed further enhanced targeting activity to angiogenic vessels in comparison to PRP-PEG-Lip or NGR-PEG-Lip along with the result from the *in vitro* association experiment. Thus, the association

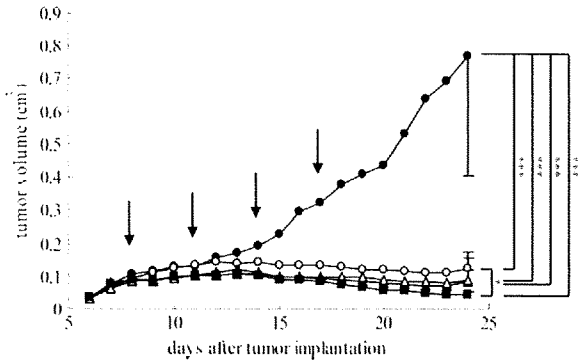

Fig. 5. Therapeutic effect of Dual-PEG-DOX in tumor-bearing mice. Colon26 NL-17-bearing mice ($n = 5$) were intravenously injected with PBS (closed circles), PEG-DOX (open circles), PRP-PEG-DOX (closed triangles), NGR-PEG-DOX (open triangles) or Dual-PEG-DOX (closed squares) at days 8, 11, 14 and 17 after tumor implantation. Injected dose of liposomal DOX were 3 mg/kg as DOX in each administration. Tumor volume and body weight (data not shown) of tumor-bearing mice were monitored. Data represent the mean tumor volume and SD, where the SD bars are shown only for the last points (day 24). Arrows show the days of injection. Asterisks show the significant differences: $^{*}P < 0.05$ and $^{***}P < 0.001$.

with angiogenic vessels *in vivo* was also improved effectively by use of dual-targeting liposomes. In our previous studies, we demonstrated that DOX encapsulated in angiogenic vessel-targeted liposomes was localized exclusively to angiogenic endothelial cells and damaged them [25]. Finally the therapeutic effect of Dual-PEG-DOX against the solid tumor was examined. Our data showed that Dual-PEG-DOX strongly suppressed the tumor growth compared with other formulations due to their potent targeting ability to angiogenic vessels. The therapeutic effects of Dual-PEG-DOX might be further enhanced by adjusting the amount of DOX in the liposomes. These findings give enough evidences for usefulness of dual-targeting liposomes in ANET.

From the result obtained in this study, it would be expected that "dual-targeting" is a useful targeting strategy for ANET. For example, combination of peptides used here and RGD would be promising approach. In addition, the investigation about the rate of peptides on dual-targeting liposomal surface would be interesting since we modified an equal amount of APRPG and GNGRG as a tentative rate. The most notable finding presented here is the fact that the targeting ability of liposomes was enhanced by dual-targeting. Dual-targeting would be available for a number of targeting therapies because most of target organs express multiple address molecules.

Conflicts of interest

None declared.

Acknowledgement

This research was supported by Grant-in-Aid for Scientific Research on Priority Areas.

Appendix A. Supplementary material

Supplementary data associated with this article can be found, in the online version, at doi:10.1016/j.canlet.2009.06.008.

References

[1] T. Sakakibara, F.A. Chen, H. Kida, K. Kunieda, R.E. Cuenca, F.J. Martin, R.B. Bankert, Doxorubicin encapsulated in sterically stabilized liposomes is superior to free drug or drug-containing conventional liposomes at suppressing growth and metastases of human lung tumor xenografts, Cancer Res. 56 (1996) 3743–3746.
[2] D.D. Lasic, Doxorubicin in sterically stabilized liposomes, Nature 380 (1996) 561–562.
[3] Y. Matsumura, H. Maeda, A new concept for macromolecular therapeutics in cancer chemotherapy: mechanism of tumoritropic accumulation of proteins and the antitumor agent smancs, Cancer Res. 46 (1986) 6387–6392.
[4] F.M. Muggia, Doxorubicin-polymer conjugates: further demonstration of the concept of enhanced permeability and retention, Clin. Cancer Res. 5 (1999) 7–8.
[5] J.W. Park, K. Hong, D.B. Kirpotin, O. Meyer, D. Papahadjopoulos, C.C. Benz, Anti-HER2 immunoliposomes for targeted therapy of human tumors, Cancer Lett. 118 (1997) 153–160.
[6] X.B. Xiong, Y. Huang, W.L. Lu, X. Zhang, H. Zhang, T. Nagai, Q. Zhang, Intracellular delivery of doxorubicin with RGD-modified sterically stabilized liposomes for an improved antitumor efficacy: in vitro and in vivo, J. Pharm. Sci. 94 (2005) 1782–1793.
[7] C. Brignole, D. Marimpietri, C. Gambini, T.M. Allen, M. Ponzoni, F. Pastorino, Development of Fab' fragments of anti-GD(2) immunoliposomes entrapping doxorubicin for experimental therapy of human neuroblastoma, Cancer Lett. 197 (2003) 199–204.
[8] F. Pastorino, C. Brignole, D. Marimpietri, P. Sapra, E.H. Moase, T.M. Allen, M. Ponzoni, Doxorubicin-loaded Fab' fragments of anti-disialoganglioside immunoliposomes selectively inhibit the growth and dissemination of human neuroblastoma in nude mice, Cancer Res. 63 (2003) 86–92.
[9] O. Ishida, K. Maruyama, H. Tanahashi, M. Iwatsuru, K. Sasaki, M. Eriguchi, H. Yanagie, Liposomes bearing polyethyleneglycol-coupled transferrin with intracellular targeting property to the solid tumors in vivo, Pharm. Res. 18 (2001) 1042–1048.
[10] J. Folkman, P.A. D'Amore, Blood vessel formation: what is its molecular basis?, Cell 87 (1996) 1153–1155
[11] M.S. O'Reilly, L. Holmgren, C. Chen, J. Folkman, Angiostatin induces and sustains dormancy of human primary tumors in mice, Nat. Med. 2 (1996) 689–692.
[12] M. Skobe, P. Rockwell, N. Goldstein, S. Vosseler, N.E. Fusenig, Halting angiogenesis suppresses carcinoma cell invasion, Nat. Med. 3 (1997) 1222–1227.
[13] T. Browder, C.E. Butterfield, B.M. Kraling, B. Shi, B. Marshall, M.S. O'Reilly, J. Folkman, Antiangiogenic scheduling of chemotherapy improves efficacy against experimental drug-resistant cancer, Cancer Res. 60 (2000) 1878–1886.
[14] N. Oku, T. Asai, K. Watanabe, K. Kuromi, M. Nagatsuka, K. Kurohane, H. Kikkawa, K. Ogino, M. Tanaka, D. Ishikawa, H. Tsukada, M. Momose, J. Nakayama, T. Taki, Anti-neovascular therapy using novel peptides homing to angiogenic vessels, Oncogene 21 (2002) 2662–2669.
[15] R.K. Jain, Normalizing tumor vasculature with anti-angiogenic therapy: a new paradigm for combination therapy, Nat. Med. 7 (2001) 987–989.
[16] T. Asai, K. Shimizu, M. Kondo, K. Kuromi, K. Watanabe, K. Ogino, T. Taki, S. Shuto, A. Matsuda, N. Oku, Anti-neovascular therapy by liposomal DPP-CNDAC targeted to angiogenic vessels, FEBS Lett. 520 (2002) 167–170.
[17] W. Arap, R. Pasqualini, E. Ruoslahti, Cancer treatment by targeted drug delivery to tumor vasculature in a mouse model, Science 279 (1998) 377–380.
[18] R. Pasqualini, E. Koivunen, R. Kain, J. Lahdenranta, M. Sakamoto, A. Stryhn, R.A. Ashmun, L.H. Shapiro, W. Arap, E. Ruoslahti, Aminopeptidase N is a receptor for tumor-homing peptides and a target for inhibiting angiogenesis, Cancer Res. 60 (2000) 722–727.
[19] E. Ruoslahti, RGD and other recognition sequences for integrins, Annu. Rev. Cell Dev. Biol. 12 (1996) 697–715.